

Characterizing multiple water-rock interactions in the critical zone through Sr-isotope tracing of surface and groundwater

Philippe Négrel, Helene Pauwels, François Chabaux

▶ **To cite this version:**

Philippe Négrel, Helene Pauwels, François Chabaux. Characterizing multiple water-rock interactions in the critical zone through Sr-isotope tracing of surface and groundwater. Applied Geochemistry, 2018, 93, pp.102-112. 10.1016/j.apgeochem.2018.04.006 . hal-03702908

HAL Id: hal-03702908
https://brgm.hal.science/hal-03702908

Submitted on 5 Dec 2022

HAL is a multi-disciplinary open access archive for the deposit and dissemination of scientific research documents, whether they are published or not. The documents may come from teaching and research institutions in France or abroad, or from public or private research centers.

L'archive ouverte pluridisciplinaire **HAL**, est destinée au dépôt et à la diffusion de documents scientifiques de niveau recherche, publiés ou non, émanant des établissements d'enseignement et de recherche français ou étrangers, des laboratoires publics ou privés.

Characterizing multiple water-rock interactions in the critical zone through Sr-isotope tracing of surface and groundwater.

Philippe NÉGREL[a, α],Hélène PAUWELS[a], François CHABAUX[b]

[a]BRGM, Orléans, France
[b]Laboratoire d'Hydrologie et de Géochimie, CNRS UMR 7517, University of Strasbourg, France.

Abstract

Here, we report on Sr isotopes, from shallow and deep groundwater from catchments located on granite and schist around the world. This extensive approach of Sr isotope tracing, initiated in France on areas impacted by intensive agricultural activities, was enlarged to Africa (granite-gneiss and schists 2200-700 Ma of the Congo Basin; Archaean granitoid/gneisses and sedimentary greenstone 3700-2500 Ma of the Orange River); India and Nepal (Archean granites 2500 Ma and Palaeoproterozoic granodiorite and schists 3100-1600 Ma for India; Himalaya metamorphic, silicate metasediments and gneisses 630 to 490 Ma); North America (3500 to 2500 Ma silicate rocks in the Mackenzie basin; 1000 to 70 Ma silicate rocks in the Fraser Basin in Canada and 1760 to 1430 Ma anorthosite and granite in the Laramie aquifer in Wyoming); South America in French Guiana (Archean gneiss 3400 to 2700 Ma and granite-gneiss rocks 2300 to 1900 Ma); Australia (65 Ma arenaceous and argillaceous rocks; and considering both surface and groundwater). In this extensive approach, the Sr and Mg contents are well correlated and both are partly related to agricultural and weathering inputs. The relationship between Sr- isotope and Mg/Sr ratios allows definition of the relative impact on surface and groundwater of processes occurring in the Critical Zone, mainly rain, agricultural practices and water-rock interactions.

Keywords: strontium isotope, critical zone, weathering, regolith

[α]Correspondingauthor:3 Avenue Claude Guillemin – BP6009 - 45060 Orléans cedex 1 – France
Tél. : +33 (0) 2 38 64 39 69 Fax : +33-(0)2 38 64 37 11
e-mail : p.negrel@brgm.fr

© 2018. This manuscript version is made available under the Elsevier user license
http://www.elsevier.com/open-access/userlicense/1.0/

1 – Introduction

The Critical Zone (CZ) is the lithosphere-atmosphere boundary where complex physical, chemical and biological processes occur and control the transfer and storage of water and chemical elements. This is the place of life-sustaining resources and where rocks release nutrients. Because it is the place where we are living, this is a fragile zone and nowadays a perturbed natural ecosystem. Surface water that drains such environments can interact with groundwater. Either surface-water bodies gain water or solutes from ground-water systems or the surface-water is a source of ground-water recharge, often causing changes in ground-water quality. Surface water and shallow groundwater are particularly vulnerable to pollution, as in many countries water resources are increasingly threatened by growing demand, wasteful use and contamination, while deeper ground resources are more protected from contamination. As climate change impacts are increasingly observed, existing challenges within science and policy are being exacerbated by the rate of change within the physical system (Ostrom, 2007). Understanding the diversity of water-rock interactions is a key issue for ensuring the CZ functioning and the geochemical characterization of different hydrological compartments (weathered rock, the weathered-fissured zone, and fractured bedrock; Larsson, 1984) involved in the water circulations. This understanding will help to predict the CZ evolution in response to environmental modifications due to tectonic, climatic or anthropogenic forcing (Brantley et al., 2007; Banwart et al., 2011).

In crystalline basement rocks; which represent more than 50% of the earth's terrestrial surface (Amiotte Suchet et al., 2003), weathering leads to the formation of a cover of an unconsolidated part named alterite or saprolite, usually representing a thickness of several tens of metres. Considering the catchment scale, the base of the alterite cover can be considered as sub-horizontal, parallel to the paleosurface contemporaneous with weathering (Fig. 1). A fissured zone develops beneath the alterite, representing a thickness of several

hundred metres. The fissuring results from rock shattering under the influence of stress generated by the swelling of certain minerals during the early stages of weathering (Wyns et al., 2004). Moreover, weathering causes the dissolution and flush of soluble cations, depending on the nature and stability of the minerals, which in turn generates mineralogical phase changes, leading in particular to the formation of clayey minerals at the expense of alumina silicates. Thus, although alterite has an interstitial porosity, their clayey mineral content means that their permeability is generally low, especially in fine-grained rocks. Conversely, the global permeability of the fissured zone is generally larger than that of the alterite, even if the permeability decreases statistically with depth in close connection to fissure density.

Water resources in hardrocks commonly involve different hydrogeological compartments such as overlying sediments, weathered rock, the weathered-fissured zone, and fractured bedrock (Larsson, 1984). Aims of the present study are to characterize the strontium isotopic ratios in watersheds or continental basins worldwide draining crystalline basement, to investigate the functioning of the different compartments of the CZ in terms of weathering processes and water pathways.

2 – Samples and methods

First, fields representing different catchments in France are used as summarized in the paper by Négrel and Pauwels (2004) and illustrated in Fig. 2: shallow and deep groundwater from granite and schist of the Armorican Massif in Brittany, northwestern France (Arguenon, Coët-Dan, Pleine-Fougeres, Négrel and Pauwels (2004); surface and shallow groundwaters from a small watershed underlain by granite or granite-gneiss in the Margeride Mountains, southern Massif Central in France (Négrel, 1999); stream- and spring-waters from the Vosges massif draining granite (NE France; Tricca et al., 1999; Probstet al., 2000; Aubert et al., 2002;

Schaffhauser et al., 2014); water flowing from the Morvan draining granite (SE Paris Basin; Négrel et al., 1988; Seimbilleet al., 1989); waters flowing in the upstream part of the Hérault watershed draining granite and mica schist (S France; Petelet,1998); and water flowing on mica schist from the Cantal (eastern Massif Central; Négrel, 1997).Other sets of samples were used: one corresponding to the Seine River draining granite (Roy et al., 1999); waters flowing in the upstream part of the Garonne River (Semhi et al., 2000); waters flowing upstream in the Pyrénées (Oliva et al., 2004); and waters flowing in the upstream part of the Moselle River (Brenot et al., 2008). These different catchments in France all drain silicate bedrocks (300-450 Ma).

We have extended to larger basins draining silicate rocks and located worldwide as illustrated in Fig. 3 for some of them: India (3a), South America (3b), Africa (3c), North America and Canada (3d), as summarized below for all considered sites:

- In India with two locations and Himalaya (Nepal). The first location in India is the Subarnarekha River Basin, located in northeastern India, rising in southern Bihar state (Négrel et al., 2007a), the river drains Precambrian metasediments, mainly mica schists, and Archean granites aged 2500 Ma. The second location in India is the Maheshwaram hydrosystem (35 km south of Hyderabad in the Ranga Reddy District, State of Andhra Pradesh). This watershed is 53 km^2 in surface area, purely endorheic and groundwater interact with Palaeoproterozoic granodiorite and schists 3100-1600 Ma (Négrel et al., 2010). In Nepal with the Himalayan rivers (the Bothe Kosi River;Harris et al., 1998) draining sillimanite-grade migmatites, gneisses and leucogranites in the upper section and kyanite–garnet metapelitic sediments in the lower sections, mid-Palaeozoic to Eocene age (450 – 50 Ma) and the Ganges headwaters (Bickle et al., 2005) that cross the major lithotectonic units of the

Himalaya (metamorphic units of the Himalayas and the silicate metasediments and gneisses of High Himalayan Crystalline Series 630 – 490 Ma in age).

- In South America with the French Guiana where the Maroni Basin (Négrel and Lachassagne, 2000) and groundwater over the whole country were investigated (Négrel and Petelet-Giraud, 2010) where weathered rocks are Archean gneiss aged 3400-2700 Ma and granite-gneiss rocks aged 2300-1900 Ma.
- In Africa with the Congo Basin with the Oubangui River (Négrel and Dupré, 1995a), the Congo River (Négrel et al., 1993; Négrel and Dupré, 1995b) and rivers draining the western part of the Congo Basin (Négrel and Dupré, 1995a). These rivers drain mainly granite-gneiss and schists, 2200-700 Ma in age. Also, in South Africa with the Orange River Basin (de Villiers et al., 2000) using the Vaal River catchment area that is underlain by granitoid/gneisses and volcano-sedimentary greenstone of the Archean Kaapvaal Basement (3700-2500 Ma) belt and below the Vaal confluence where the Orange River traverses the Namaqualand Basement Complex, lower Karoo sequences and Kalahari sands.
- In North America with the Mackenzie and Fraser Basin in Canada and the Laramie aquifer (Wyoming USA, Frost and Toner, 2004). The Mackenzie River (Slave Province, Millot et al., 2002) where rivers drain 213,000 km^2 of old crystalline basement from 3500 to 2500 Ma with silicate rocks predominating (potassium-rich rocks, gneisses) and the Fraser River (British Columbia, Cameron et al., 1995) draining 238,000km^2 and crossing through a number of geological belts (Upper Proterozoic to tertiary -1000 to 70 Ma - metamorphic and I- or S-type granitic rocks, silicate sedimentary rocks). The aquifer in the Laramie basin (Wyoming) crosses Precambrian igneous and metamorphic rocks (1760 Ma Horse Creek Anorthosite

Complex with anorthosite, monzonite, and granite, 1430 Ma Sherman Granite Batholith).

- Central Australia with groundwater from Tertiary sedimentary aquifers of the arid Ti-Tree Basin (Harrington and Herczeg, 2003). The basin is composed of a suite of arenaceous and argillaceous Cenozoic rocks (65 Ma) derived through weathering of the Proterozoic igneous and metamorphic rocks also including granite, gneiss, schist and quartzite (2500 to 540 Ma).

3 – Additional results in this study

All data compiled/reported in this paper have been already published except those from the Maheshwaram catchment in India. In this small endorheic watershed, representative of South Indian conditions in terms of geology (hard rock), land-use, overpumping of the hard-rock aquifer (over 700 bored open-end wells in use, surface waters are ephemeral and occur only during the monsoon period. Moreover, the chemical composition of groundwater is strongly impacted by evaporation linked to irrigation return flow (Perrin et al., 2011). Samples in the Maheshwaram hydrosystem (Fig. 4) were collected and analyzed in two sampling periods 2006 and 2008 (Négrel et al., 2010; Pauwels et al., 2015). The 2006 and 2008 samples were analyzed for Mg contents by ICP-AES and Sr content by ICP-MS at BRGM. The 2006 samples were analyzed for Sr isotopes at National Geophysical Research Institute NGRI, Hyderabad (A. Dayal, personal communication) whereas the 2006 samples were analyzed at Laboratoire d'HYdrologie et de GEochimie de Strasbourg LHyGeS. The Sr was separated using the classical procedure purification using ion exchange resins and the isotopic ratios were determined by thermal-ionisation mass spectrometer with an analytical uncertainty of around 20ppm (2σmean). The $^{87}Sr/^{86}Sr$ value of the NBS 987 standard was routinely measured in both labs. For more details, see Prunier et al., 2015.

Strontium content varies greatly in groundwater samples between 2.3 and 33.1 µmol/l. The range is between 2.3 and 33.10 µmol/l in 2006 and between 4.6 and 17.1 µmol/l in 2008. The observed range partly agrees with that found in groundwater in the Subarnarekha River basin with Sr contents from less than 3.4 up to 100.5 µmol/l (Négrel et al., 2007a). Strontium isotopes display a wide variation in the groundwater from 0.71606 (lower values both in 2006 and 2008) to 0.72843 observed in 2008 (0.72823 as higher value in 2006). The $^{87}Sr/^{86}Sr$ ratios observed in groundwater agrees with those of waters draining old cratons (Guyana Shield, Edmond et al., 1995; French Guiana, Négrel and Lachassagne, 2000; Lena River Basin in Russia, Huh and Edmond, 1999; Ganga-Brahmaputra-Indus River system in India, Krishnaswamiet al., 992; Pande et al., 1994; Singh et al., 1998; Dowling et al., 2003; Himalayan rivers, Galy et al., 1999).

4 - Discussion

4.1. The Sr isotope data from shallow and deep groundwater in silicate over France

Strontium isotopes are useful tracers of water-rock interaction (Blum et al., 1994; Brantley et al., 1998; Négrel et al., 2001) and of mixing of water from different origins (Roy et al., 1999; Négrel et al., 2001; Mc Nutt et al., 1990). Part of the Sr mass balance in a crystalline environment is controlled by chemical weathering of the most commonly Sr-bearing phases from the silicate host rock, either primary phases (apatite, plagioclase, K-feldspar, biotite and muscovite) or their alteration products, e.g. epidote and clay minerals (Blum et al., 1994; Brantley et al., 1998; Mc Nutt et al., 1987; Aubert et al., 2002; Pett-Ridge et al., 2009),inputs from rainwater and anthropogenic disturbance. The latter, through agricultural activity, induces an input of Sr that may be important (Négrel, 1999; Roy et al., 1999) depending on the range of Sr contents in fertilizers and carbonate additives (3–1500 µg/g) with a Sr-isotope ratio from 0.70794 to 0.7095. This range is reflected in manure from livestock, such as hogs and poultry (Sr range from 2 to 4 µg/g, $^{87}Sr/^{86}Sr$ ratio from 0.7092 to 0.71092)

Starting from data of groundwater collected in three granitic and Brioverian 'schist' aquifers of the Armorican Massif, the observed Sr content is well correlated with Mg and both are partly related to agricultural practices and water rock interaction (Fig. 5, Négrel and Pauwels, 2004). Combined with additional data from surface and groundwater of catchments draining silicate bedrocks (300-450 Ma) like the Hérault, Seine, Moselle, Garonne, Morvan, Margeride, Cantal, Pyrenees and Vosges (from the literature, Fig. 5) revealed a unique trend between Sr and Mg expressed by the relationship Mg (µmol/l) = A x Sr (µmol/l); with A varying between 100 and 600 (Fig. 5).As demonstrated before (Négrel and Pauwels, 2004), Mg is closely linked with Sr (and Cl) and therefore the variability in the Cl *vs.* Mg relationship interpreted as variations in the agricultural practices from a non-polluted status (e.g. the water rock interaction), enhanced the use of Mg/Sr ratios. The use of this ratio rather than absolute concentrations alone, avoids variations due to dilution or concentration effects and the normalization to the Sr content transforms mixing curves into straight lines (Faure, 1986).

The relationship between Sr-isotope and Mg/Sr ratios (Fig. 6) allows better definition of the different endmembers, mainly rain, agricultural practices and water-rock interaction. Actually, the 3 endmembers rain inputs, fertilizer and manure present very close characteristics with low $^{87}Sr/^{86}Sr$ and low Mg/Sr ratios (Négrel, 1999; Négrel et al., 2007b). Two binary mixing trends connect fertilizer and manure and the isotope composition of the endmembers reflecting the water rock interaction in the different compartments. This implies the occurrence of (i) high $^{87}Sr/^{86}Sr$ and low Mg/Sr ratios, and (ii) low $^{87}Sr/^{86}Sr$ and high Mg/Sr ratios endmembers, which could be related to different water rock interaction conditions. Water originating from the upper compartment of the aquifer in weathered rock (alterite) is one of the water rock interaction endmembers. The interaction of water with alterite thus led to higher $^{87}Sr/^{86}Sr$ ratios in the water because of the weathering of residual

minerals (Bullen et al., 1997; Négrel, 1999). It is worth noting that the Vosges waters may represent partly such a compartment with regard to the $^{87}Sr/^{86}Sr$ and Mg/Sr ratios. Water from the lower compartment of the aquifer, mainly comprising fissured fresh rock, constitutes the second water rock interaction endmember. Interaction in the fissured part implies that the Sr-isotope characteristics of waters are more related to the weathering of whole rock (e.g. a lower $^{87}Sr/^{86}Sr$ ratio: Négrel, 1999; Négrel and Pauwels, 2004).

All ground- and surface waters for catchments draining silicate bedrocks are scattered between at least three geochemical signatures with some particular points plotting close to the different mixing lines. This is the case for the Garonne, Seine, Pyrénées and to a lesser degree for the Morvan, Cantal and Vosges (Négrel et al., 1988; Roy et al., 1999; Probst et al., 2000; Aubert et al., 2002; Pierret et al., 2014), and Margeride field (Négrel, 1999), which are in an intermediate location along the mixing line between fertilizer and manure and the endmember corresponding to alterite. The intermediate location suggests influences from either agricultural practices (Négrel, 1999; Roy et al., 1999) or rain, the latter being less probable. Regarding Brittany, high Mg/Sr samples from the Coet-Dan catchment plot along the mixing line between fertilizer and manure and the endmember corresponding to the fissured part of the aquifer, comprising fresh rock whereas high Mg/Sr samples from the Plaine-Fougères and Arguenon catchments plot along and/or near the mixing line between the two WRI endmembers. These locations reflect the relative lack of anthropogenic contribution to Sr content compared to water-rock interactions and, in the case of Arguenon, the occurrence of waters corresponding to a mixing between upper and lower compartments of the aquifer. The Plaine-Fougères field defines a linear trend towards the pollution endmember, with the low$^{87}Sr/^{86}Sr/$ and Mg/Sr ratios of this field in agreement with the characteristics of the Hérault upstream waters (Petelet, 1998), thus reflecting considerable anthropogenic input in the upper part of the Hérault catchment as suggested by Petelet (1998). The Vosges (Probst et al., 2000;

Aubert et al., 2002; Pierret et al., 2014; Schaffhauser et al., 2014) partly agree with the alterite endmember but some waters are marked by the endmember corresponding to the fissured part of the aquifer as they plot near the mixing line between the upper and lower parts of the aquifer.

4.2. Extensive approach using Sr isotope in surface and groundwater in the critical zone

4.2.1 The focus on the Maheshwaram hydrosystem

The fluctuations of the Sr contents in the endorheic Maheshwaram hydrosystem are correlated with those of Cl by the equation Cl = 0.14 x Sr - 36.06 (N = 39, R^2 = 0.67). This relationship suggests that the source of chloride is also a potential source of Sr that can be related to agricultural practices (Atal et al., 2010) as the bedrock is only comprised of silicates (e.g., granite).

The Sr-isotope studies of water have shown that variations in Sr isotopes are primarily caused by mixing of waters of various origins with different $^{87}Sr/^{86}Sr$ ratios and Sr contents such as mixing between different water pools, each of them possibly reflecting water-rock interaction with different rock types or different stage of water rock interaction in the same bedrock. A comparison of the $^{87}Sr/^{86}Sr$ *vs.* Cl and Sr contents shows that all the water samples from the Maheshwaram hydrosystem are largely scattered with regard to both Sr isotopes and Sr concentrations. Comparing the Sr isotope ratios and the chloride contents argues in favour of three endmembers as samples are scattered in three directions (Fig. 7a). Rainwater inputs display low Cl contents in the Maheshwaram hydrosystem, around 113 µmol/l (Négrel et al., 2011) and anthropogenic inputs show the highest Cl contents, up to 7042 µmol/l, and the natural background (e.g. the water rock interaction) has a low Cl content, near that of rainwater. The most dilute endmember in Fig. 7a could be rainwater inputs for which characteristics are usually a $^{87}Sr/^{86}Sr$ ratio ranging between 0.714 to 0.720 (Galy et al., 1999; Négrel et al., 2007a), and Cl contents around 113 to 563 µmol/l. With a mean weighted

chloride content of 25 µmol/l in rainwater and the concentration factor related to the quantity of precipitation and the evaporation rate, a maximum for rain-derived Cl of 225 to 563 µmol/l was determined (Négrel et al., 2011), in agreement with the range observed for this endmember. The most mineralised endmember has a broader range of Sr isotope ratios from 0.71609 to 0.72769 and Cl contents in the range 7296-8028 µmol/l. This second endmember is believed to correspond to anthropogenic inputs, mainly agricultural in origin (livestock farming, fertilizer spreading and partly related to domestic sewage and in situ sanitation). The third endmember is characterised by a $^{87}Sr/^{86}Sr$ ratio ranging between 0.72796 and 0.72843 and a Cl content around 563 - 1408 µmol/l. This range of Cl contents agrees with the rain-derived Cl as stated above and corresponds to water rock interaction.

A comparison of the $^{87}Sr/^{86}Sr$ *vs.* Sr contents shows that all the water samples from the Maheshwaram hydrosystem are largely scattered with regard to both Sr isotopes and Sr contents. It is worth noting that (1) the large variation in the Sr contents corresponds to the highest $^{87}Sr/^{86}Sr$ ratios and (2) the relatively restricted range of the Sr contents in the lowermost values corresponds to large variations in $^{87}Sr/^{86}Sr$ ratios. Illustrated in a diagram of $^{87}Sr/^{86}Sr$ ratios *vs.* 1/Sr (Fig. 7b), the endmembers defined in Fig. 7a cannot be fully used. Two endmembers can be considered, meaning the endmember corresponding to anthropogenic inputs with high Sr contents and variable $^{87}Sr/^{86}Sr$ ratio and the endmember corresponding to water rock interaction with a high $^{87}Sr/^{86}Sr$ ratio and large Sr content variations. The endmember previously related to rain inputs cannot be considered here as the Sr contents in the groundwater are too large compared to the values for the rain inputs (Sr content around 1µg/l, Négrel et al., 2007a). This implies the existence of a second endmember corresponding to water-rock interaction with a restricted range in Sr content and a $^{87}Sr/^{86}Sr$ ratio close to 0.715 (Fig. 7b). Such variations in the $^{87}Sr/^{86}Sr$ *vs.*Sr contents in groundwater

issued from a similar granitic catchment, and related to changes in water-rock interactions, have been observed by Négrel et al. (2000).

4.2.2 The extensive approach by enlarging to worldwide basins and catchments

An extensive approach was done by enlarging to Africa (granite-gneiss and schists 2200-700 Ma of the Congo Basin; Négrel et al. 1993;Archaean granitoid/gneisses and sedimentary greenstone 3700-2500 Ma of the Orange River; de Villiers et al., 2000);India and Nepal (Archean granites 2500 Ma and Palaeoproterozoic granodiorite and schists 3100-1600 Ma, Négrel et al., 2007a and this study for India; Himalaya metamorphic, silicate metasediments and gneisses 630 to 490 Ma; Harris et al., 1998; Bickle et al., 2005); North America (3500 to 2500 Ma silicate rocks in the Mackenzie basin; Millot et al., 2002 and 1000 to 70 Ma silicate rocks in the Fraser Basin in Canada; Cameron et al., 1995 and1760 to 1430 Ma anorthosite and granite in the Laramie aquifer in Wyoming; Frost and Toner, 2004); South America in French Guiana (Archean gneiss 3400 to 2700 Ma and granite-gneiss rocks 2300 to 1900 Ma; Négrel and Petelet-Giraud, 2010); Australia (65 Ma arenaceous and argillaceous rocks; and considering both surface and groundwater; Harrington and Herczeg, 2003).

In a way identical to observations made at the scale of France, the Sr content is well correlated with Mg as illustrated in Fig. 8, when enlarging to worldwide basins and catchments. The highest values are observed in India in the Maheshwaram watershed (this study) where more than 700 boreholes are used for agricultural irrigation in this endorheic watershed of 53 km^2 surface area. The second place in India (the Subarnarekha River Basin), also with high agricultural activities, has high Sr-Mg contents (Négrel et al., 2007a), however with a lower range then that observed in the Maheshwaram watershed. Also, in South Africa with the Orange River Basin the high contents in these elements are related, according to de Villiers et al. (2000), to agricultural practices. The Ti-Tree Basin in Central Australia also has groundwater with high Sr-Mr contents. As this is a very arid part of the Australian country

with a ratio of mean annual rainfall over potential evaporation of less than 0.1 (Harrington and Herczeg, 2003), the groundwater resource is intensively used for a small but lucrative horticulture industry, thus inducing the high Sr-Mg contents. Contrary to the zones where the high Sr-Mg contents are related to larger agricultural practices, the lowest values are observed in French Guiana and Africa (Congo and Congo occidental basin, Oubangui) where rain inputs and water rock interactions are predominant processes. The rest of the studied sites are scattered between low and high Sr-Mg contents as representing a mix between rain inputs, water-rock interaction and anthropogenic inputs.

The weathering processes studied here all focus on old silicate environments, with ages up to 3100 Ma, such weathered silicates therefore yield clearly larger ranges in the Sr-isotope ratios as illustrated in Fig.9 when compared to the Mg/Sr ratio. The lowest $^{87}Sr/^{86}Sr$ value being observed in the Congo Basin (Kouilou river, Négrel and Dupré, 1995a, b), in French Guiana (Négrel and Lachassagne, 2000; Négrel and Petelet-Giraud, 2010) and in the Fraser River basin (Cameron et al., 1995). The higher $^{87}Sr/^{86}Sr$ value (up to 0.765) being observed in Australia (Harrington and Herczeg, 2003) as other high values are observed in in the Ganga headwaters (0.7526 and 0.7489,Bickle et al., 2005), in the Fraser river Basin (0.7513, Cameron et al., 1995) and in groundwater from Finland draining tills developed on granites (0.7508, Négrel et al., 2005). The Sr-isotopes tracing the origin of dissolved compounds define and identify the circulation pathways of waters and compare to the former plot with the French sites, the additional data define a large scatter for the Sr- isotope ratios.

More detail in Fig. 9, the scattering of the data sets from *India* is between alterite and rain or agricultural practices for Maheshwaram site and between the three endmembers (alterite, underlying weathered-fissured and fractured bedrock and rain or agricultural practices) for the Subarnarheka site reflecting the larger influence of deep alteration processes in the water in this area (Négrel et al., 2007a). For the Himalayan rivers, the Bothe Kosi River

(Harris et al., 1998) has scatteredSr-isotope ratios ranging between 0.7187 and 0.7409 and a low Mg/Sr (145 – 208) that reflects a mixing between the alterite compartment and agricultural practices (also reflected by the range of Sr – Mg contents). The Ganges headwaters (Bickle et al., 2005) are scattered between the three endmembers, one sample with high Sr – Mg content displays the lowest $^{87}Sr/^{86}Sr$ ratio reflecting a large contribution of the anthropogenic endmember. The other samples reflect the influence of the alterite endmember with increasing $^{87}Sr/^{86}Sr$ ratio (up to 0.7526) combined with Mg/Sr ratio in the range 120 – 220. One sample appears to be a mix between the alterite compartment and underlying weathered-fissured and fractured bedrock as the sample plots along the mixing line between these two endmembers with a Mg/Sr ratio of 470 and a$^{87}Sr/^{86}Sr$ ratio of 0.7489.

In *Africa*, the scattering of the surface water data in the Congo Basin lies between the three endmembers: rain inputs as previously evidenced by Négrel et al. (1993, 1995a, b) but also the alterite compartment and underlying weathered-fissured and fractured bedrock. The weak influence of agricultural practices is confirmed by the low Sr-Mg values (Fig. 8). For the Oubangui basin (Négrel and Dupré, 1995a), the alterite compartment has a strong influence on the groundwater while the surface waters are scattered between the three endmembers with a stronger influence of underlying weathered-fissured and fractured bedrock. For the Congo Basin (Fig. 2c), both the yearly survey at Brazzaville (Négrel and Dupré, 1995b) and the investigation at the basin scale (Négrel et al., 1993) show a strong influence of the rain inputs and underlying weathered-fissured and fractured bedrock reflecting the groundwater influence with an increase of the Mg/Sr ratio during low water stage and slight decrease of the $^{87}Sr/^{86}Sr$ ratio. Rivers draining the western part of the Congo Basin (Négrel and Dupré, 1995a) show a strong influence of the alterite and underlying weathered-fissured and fractured bedrock as most of the samples plot along the mixing line between these two endmembers. In South Africa, the Orange River Basin is marked by a

strong influence of agricultural practices as confirmed by the relatively high Sr-Mg values but also the alterite compartment and a weak influence of underlying weathered-fissured and fractured bedrock with a Mg/Sr ratio remaining around 350.

In *French Guiana,* the scatter of the data is between the three endmembers. In the surface waters collected during low water stage the data clearly reflect the influence of the alterite for some samples (Négrel and Lachassagne, 2000), the influence of rain inputs for others (no water rock interaction as shown by Négrel and Petelet-Giraud, 2010) and the influence of underlying weathered-fissured and fractured bedrock for the rest. Regarding the groundwater, there is less influence of the alterite compartment and the data being scattered between the rain inputs and the underlying weathered-fissured and fractured bedrock as demonstrated by Négrel and Petelet-Giraud (2010).

In *North America*, regarding the Mackenzie River basin in Canada, scatter of the data is between the three endmembers reflecting the prominent influence of the alterite and rain inputs and less influence of underlying weathered-fissured and fractured bedrock. The role of anthropogenic endmembers can be discarded as illustrated by the lowSr-Mg values (Fig. 8). Most of the samples from the Fraser Basin in Canada plot between the anthropogenic inputs and the alterite compartment with less influence of the latter. It is worth noting the location of one sample along the mixing line between the alterite compartment and the underlying weathered-fissured and fractured bedrock. In the Laramie aquifer (Wyoming USA), one sample plots close to the weathered-fissured and fractured bedrock whereas the second one is marked by the three endmembers, reflecting a more prominent role of the alterite and less from anthropogenic inputs.

In *Australia* (Harrington and Herczeg, 2003), the groundwaters are scattered along the mixing line between the alterite compartment and the anthropogenic inputs reflecting a more

prominent role of the weathering processes in the alterite and the lack of any influence of deeper interaction of the weathered-fissured and fractured bedrock.

Groundwaters from *Finland* are close to the field defined in the Mackenzie River basin in Canada reflecting again the prominent influence of the alterite and rain inputs and less influence of underlying weathered-fissured and fractured bedrock and anthropogenic endmembers (as illustrated by the low Sr-Mg values in Fig. 8).

4.2.3 Variation in the alterite endmember: a consequence of bedrock age?

Through the use of different databanks of ground- and surface waters collected worldwide, we have illustrated large variations in Sr-isotope ratios with variations in the Mg/Sr ratios (Fig. 5, 8 and 9). Evidence of such co-variation has not previously been reported for isotopic ratios of Sr at this scale, and this result highlights the impact of the degree of silicate weathering on strontium isotopes due to different water-rock interaction processes.

In silicate rocks, a pattern is generally observed of increasing $^{87}Sr/^{86}Sr$ in the order plagioclase, hornblende, K-feldspar, and biotite, in close connection with the Rb/Sr ratio of each mineral. Meaning that minerals having a high Rb/Sr will have greater $^{87}5r/^{86}Sr$ than minerals having low Rb/Sr because the ^{87}Rb decays to ^{87}Sr with a half-life of 48.8 billion years. The preferential alteration of strontium-rich, rubidium-poor minerals during weathering causes the increase of the Rb/Sr ratio in weathered rock compared to the Rb/Sr ratio of the fresh rock (Dasch, 1969) and thus the increase in $^{87}Sr/^{86}Sr$ ratios in the bulk alterite can be related with weathering removal over time of the remaining nonradiogenic plagioclase, apatite and hornblende (Pett-Ridge et al., 2009). This relative enrichment of rubidium over strontium is evident in most weathering profiles (Dasch, 1969) and continuous interaction in the alterite thus led to high Sr-isotope ratios in waters because of the weathering of residual minerals. However, in addition to the role of the Rb/Sr ratio, the age of rocks, in connection with decay,

promotes high ratios in minerals having high Rb/Sr. This means that for alterite developed on silicate rocks, older the rocks are, the more radiogenic the residual minerals are.

Interactions within the alterite of silicate in France, mainly having an age of approximately 300 to 400 Ma show lower isotope ratios as proved by comparison of water samples representing this horizon when comparing to those having older age like Vosges in France and Australia for example. These interactions in alterite of different ages can be modified by the impact of agricultural inputs (Africa, Laramie aquifer in Wyoming USA, Australia, …) or rain inputs (Himalaya, French Guiana, Mackenzie River basin in Canada, Finland…). In water in which we may state that Sr and Mg are mostly of natural sources, but due to human pressures, Sr and its isotopes are not an excellent tracer of natural processes. However, we have demonstrated that all considered sites, Sr isotopes can serve as a tracer of water-rock interaction in the context of silicate weathering.

5 – Conclusion

Strontium isotopic tracers allow the water-rock interaction and complex relationships between the different compartments of hard-rock aquifers to be more clearly defined, from small-scale catchments to the scale of continental basins, using data acquired from sites worldwide. The existence of relatively deep alteration processes, whose role in the functioning of the critical zone will have to be properly taken into account in future studies, i.e. regarding the leaching of toxic element such as fluorides (Pauwels et al., 2015) or water pathways (Chabaux et al., 2017), is evidenced by tracing Sr isotopes. The contrasting strontium-isotope signatures are linked to differences in weathered mineral phases of the bedrock regardless of the age of the geological formations. The ground- or surface waters can show either an increase or a decrease in the proportions of weathered phases, which probably are related to the functioning of the weathering profile in crystalline rock (Dasch,

1969; Négrel, 1999; Probst et al., 2000). The Sr-isotope tracing defines and identifies the relative signature of water circulation in alterite and underlying weathered-fissured and fractured bedrock. Due to its large range in abundance of the residual minerals, the alterite endmember has Sr isotope ratios that may vary as a function of the age of the bedrock. Effective water management is considered crucial for building adaptive capacity to be resilient to the impacts of climate change (Nelson et al., 2007). Thus, a greater understanding of the nature of weathering processes involved and their relationships with water circulation is seen as being at the heart of present and future water challenges (Négrel and Petelet-Giraud, 2013).

Acknowledgements

The study of the Maheshwaram watershed was carried out at the Indo-French Centre for Groundwater Research (BRGM-NGRI) supported by French Research National Agency (ANR) through VMCs program (project MOHINI no. ANR-07-VULN-08) and by the BRGM research Division through the project "Isotopes". The authors thank the French Ministry of Foreign Affairs and the French Embassy in India for their support.

Chemical and isotopic analyses were performed in the geochemistry Laboratory of BRGM, France. The work benefited from the collaboration of C. Guerrot (BRGM Mass-Spectrometer team), who provided the strontium isotope analyses and T. Conte (BRGM Environmental Chemistry team) who provided the chemical analyses. R. Wanty (USGS) is warmly thanked for the critical comments and constructive review that greatly improved the manuscript and for proofreading and editing the English text.

References

Amiotte Suchet, P., Probst, J.-L., Ludwig, W. 2003.Worldwide distribution of continental rock lithology: Implications for the atmospheric/soil CO_2 uptake by continental weathering and alkalinity river transport to the oceans, Global Biogeochem. Cycles, 17, 1038, DOI 10.1029/2002GB001891.

Atal, S., Négrel, Ph., Pauwels, H., Mascré, C., Ahmed, S. 2010. Double correction technique for characterising groundwater quality zones: a case study from granitic setting, India. Water Qual Expo Health. DOI 10.1007/s12403-010-0031-6.

Aubert, D., Probst, A., Stille, P., Viville, D. 2002. Evidence of hydrological control of Sr behavior in stream water (Strengbach catchment, Vosges mountains, France). App. Geochem. 17(3), 285-300.

Banwart, S., Bernasconi, S.M., Bloem, J., Blum, W., Brandao, M., Brantley, S.,Chabaux, F., Duffy, C., Kram, P., Lair, G., Lundin, L., Nikolaidis, N., Novak, M., Panagos, P., Ragnarsdottir, K.V., Reynolds, B., Rousseva, S., de Ruiter, P., van Gaans, P., van Riemsdijk, W., White, T., Zhan, B. 2011. Soil processes and functions in critical zone observatories: hypotheses and experimental design. Vadose Zone J., 10, 974–987.

Bickle, M. J., Chapman, H. J., Bunbury, J., Harris, N. B., Fairchild, I. J., Ahmad, T., Pomiès, C. 2005. Relative contributions of silicate and carbonate rocks to riverine Sr fluxes in the headwaters of the Ganges. Geochim. Cosmochim. Acta, 69, 2221-2240.

Blum, J.D., Erel, Y., Brown, K. 1994, $^{87}Sr/^{86}Sr$ ratios of Sierra Nevada stream waters: Implications for relative mineral weathering rates. Geochim. Cosmochim. Acta 58, 5019–5025.

Brantley, S.L., Chesley, J.T. Stillings, L.L. 1998. Isotopic ratios and release rates of strontium measured from weathering feldspars. Geochim. Cosmochim. Acta 62, 1493–1500.

Brantley, S.L., Goldhaber, M.B., Ragnarsdottir, K.V. 2007. Crossing disciplines and scales to understand the critical zone. Elements 3, 307-314.

Brenot, A., Cloquet, C., Vigier, N., Carignan, J., France-Lanord, C. 2008. Magnesium isotope systematics of the lithologically varied Moselle river basin, France. Geochim. Cosmochim. Acta 72, 5070–5089.

Bullen, T., White, A., Blum, A., Harden, J., Schulz, M. 1997. Chemical weathering of a soil chronosequence on granitoid alluvium: II. Mineralogic and isotopic constraints on the behavior of strontium. Geochim. Cosmochim. Acta 61, 291-306.

Cameron, E.M., Hall, G.E.M., Veizer, J., Krouse, H.R. 1995. Isotopic and elemental hydrogeochemistry of a major river system: Fraser River, British Columbia, Canada. Chem. Geol. 122, 149-169.

Chabaux, F., Viville, D., Aquilina. L., Lucas, Y., Ackerer, J., Ranchoux, C., Bosia, C., Pierret, M.C., Labasque, T., Lerouge, C., Dezayes, C., Négrel, Ph. 2017. Geochemical tracing and modeling of surface and deep water-rock interactions in elementary granitic watersheds

(Strengbach and Ringelbach CZOs, France). Acta Geochim. DOI :10.1007/s11631-017-0163-5.

Dasch, E.J. 1969. Strontium isotopes in weathering profiles, deep-sea sediments, and sedimentary rocks. Geochim. Cosmochim. Acta 33, 1521-1552.

de Villiers, S., Compston, J.S., Lavelle, M. 2000. The strontium isotope systematics of the Orange River, Southern Africa. South African J. Geol. 103, 237-248.

Dowling, C.B., Poreda, R.J., Basu, A.R. 2003. The groundwater geochemistry of the Bengal Basin: weathering, chemsorption, and trace metal flux to the oceans. Geochim Cosmochim Acta 67, 2117–2136.

Edmond, J.M., Palmer, M.R., Measures, C.I., Grant, B., Stallard, R.F. 1995. The fluvial geochemistry and denudation rate of the Guayana shield in Venezuela. Geochim Cosmochim Acta 59, 3301–3325.

Faure, G., 1986. Principles of Isotope Geology. Wiley, New York, p. 589.

Frost, C.D., Toner, R.N. 2004. Strontium Isotopic Identification of Water- Rock Interaction and Ground Water Mixing. Groundwater, 42, 418-432.

Galy, A., France-Lanord, C., Derry, L.A. 1999. The strontium isotopic budget of Himalayan rivers in Nepal and Bangladesh. Geochim Cosmochim Acta 63, 1905–1925.

Harrington, G.A., Herczeg, A.L. 2003. The importance of silicate weathering of a sedimentary aquifer in arid Central Australia indicated by very high $^{87}Sr/^{86}Sr$ ratios. Chem. Geol. 199, 281-292.

Harris, N., Bickle, M., Chapman, H., Fairchild, I., Bunbury, J. 1998. The significance of Himalayan rivers for silicate weathering rates: evidence from the BhoteKosi tributary. Chem. Geol. 144 1998 205–220.

Huh, Y., Edmond, J.M. 1999. The fluvial geochemistry of the rivers of Eastern Siberia: III. tributaries of the Lena and Anabar draining the basement terrain of the Siberian Craton and the Trans-Baikal Highlands. Geochim. Cosmochim. Acta 63, 967–987.

Krishnaswami, S., Trivedi, J.R., Sarin, M.M., Ramesh, R., Sharma, K.K. 1992. Strontium isotopes and rubidium in the Ganga-Brahmaputra river system: weathering in the Himalaya, fluxes to the Bay of Bengal and contributions to the evolution of oceanic $^{87}Sr/^{86}Sr$. Earth Planet. Sci. Let. 109, 243–253.

Larsson, I. 1984. Ground water in hard rocks. Unesco. 234pp.

McNutt, R.H., Gascoyne, M., Kamineni, D.C., 1987. $^{87}Sr/^{86}Sr$ values in groundwaters of the East Bull Lake pluton, Superior Province, Ontario, Canada. App. Geochem. 2, 93–101.

McNutt, R.H., Frape, S.K, Fritz, P., Jones, M.G., MacDonald, I.M., 1990. The $^{87}Sr/^{86}Sr$ values of Canadian Shield brines and fracture minerals with applications to groundwater mixing, fracture history, and geochronology. Geochim. Cosmochim. Acta 54, 205–215.

Millot, R., Gaillardet, J., Dupré, B., Allègre, C.J. 2002. The global control of silicate weathering rates and the coupling with physical erosion: new insights from rivers of the Canadian Shield. Earth Planet. Sci. Let. 196, 83-98.

Négrel, Ph., Dupré, B., Seimbille, F., Allègre, C.J. 1988. Quantitative modelling of differential erosion between crystalline and sedimentary area of a French basin by isotopic analysis of strontium in river waters. European Association for Geochemistry, Paris 1988. Chem. Geol. 70, 13.

Négrel, Ph., Allègre, C.J., Dupré, B., Lewin, E. 1993. Erosion sources determined from inversion of major, trace element ratios and strontium isotopic ratios in river water: the Congo Basin case. Earth Planet. Sci. Lett., 120, 59-76.

Négrel, Ph., Dupré, B. 1995a. Temporal variations of strontium isotopic ratios of the Oubangui river basin: Implications for the sources of material. Colloques et Séminaires de l'ORSTOM, Grands Bassins Fluviaux, 181-198.

Négrel, Ph., Dupré, B. 1995b. Seasonal fluctuations of major, trace elements composition and Sr isotopic ratios at the Congo Basin outcrop during 1989. Implications for the hydrological functionning. Colloques et Séminaires de l'ORSTOM, Grands Bassins Fluviaux, 39-50.

Négrel, Ph. 1997. Traçage des apports anthropiques sur un petit bassin versant: Utilisation des rapports isotopiques du strontium. Comptes rendus de l'Académie des Sciences, Paris 4, Série II, 907–914.

Négrel, Ph. 1999. Geochemical study of a granitic area – The Margeride Mountains, France: Chemical element behavior and $^{87}Sr/^{86}Sr$ constraints. Aquat. Geochem. 5, 125–165.

Négrel, Ph., Lachassagne, P. 2000. Geochemistry of the Maroni River (French Guyana) during low water stage: Implications for water rock interaction and groundwater characteristics. J. Hydrol., 237, 212-233.

Négrel, Ph., Guerrot, C., Cocherie, A., Azaroual, M., Brach, M., Fouillac, Ch. 2000. Rare earth elements, neodymium and strontium isotopic systematics in mineral waters: evidence from the Massif Central, France App. Geochem. 15, 1345-1367.

Négrel, Ph., Casanova, J., Aranyossy, J.F. 2001, Strontium isotope systematics used to decipher the origin of groundwaters sampled from granitoids: The Vienne case (France). Chem. Geol. 177, 287–308.

Négrel, Ph, Pauwels, H, 2004. Interaction between different groundwaters in Brittany catchments (France): characterizing multiple sources through strontium- and sulphur isotope tracing. WASP. 151, 261-285.

Négrel, Ph., Casanova, J., Blomqvist, R, 2005. $^{87}Sr/^{86}Sr$ of brines from the Fennoscandian Shield: a synthesis of groundwater isotopic data from the Baltic Sea region. Can. J. Earth Sci. 42, 273–285.

Négrel, Ph., Machard de Gramont, H, Lemière, B, Billaud, P, Sengupta, B, 2007a. Hydrogeochemical processes, mixing and isotope tracing in hard rock aquifers and surface waters from the Subarnarekha River basin, (east Singhbhum district, Jharkhand state India). Hydrogeol. J., 15, 1535-1552.

Négrel, Ph., Guerrot, C., Millot, R., 2007b. Chemical and strontium isotope characterization of rainwater in France: influence of sources and hydrogeochemical implications. Isotopes Environ. Health Studies 43, 179–196.

Négrel, Ph, Petelet-Giraud, E, 2010. Geochemistry and isotopic composition (O, D, Sr, Nd) in the groundwater of French Guiana as indicators of their origin and interrelation. Geosciences, 342, 786-795.

Négrel, Ph, Millot, R., Roy, S., Guerrot, C., Pauwels, H. 2010. Lead isotopes in groundwater as an indicator of water–rock interaction (Masheshwaram catchment, Andhra Pradesh, India). Chem. Geol. 274, 136–148.

Négrel, Ph, Pauwels, H., Dewandel, B., Gandolfi, J.M., Mascré, C., Ahmed, S. 2011. Understanding groundwater systems and their functioning through the study of stable water isotopes in a hard-rock aquifer (Maheshwaram watershed, India). J. Hydrol. 397, 55–70.

Négrel, Ph., Petelet-Giraud, E., 2013. Isotopes in groundwater as indicators of climate changes. TrAC 30, 1279-1290.

Nelson, D.R., Adger, W.N., Brown, K. 2007. Adaptation to environmental change: contributions of a resilience framework. Annual Review of Environment and Resources 32, 395-419.

Oliva, P., Dupre, B., Martin F. Viers, J. 2004. The role of trace minerals in chemical weathering in a high-elevation granitic watershed (Estibere, France): Chemical and mineralogical evidence. Geochim. Cosmochim. Acta, 68, 2223–2244.

Ostrom, E, 2007. A diagnostic approach for going beyond panaceas. Proceedings of the National Academy of Sciences of United States of America 104, 419-422.

Pande, K., Sarin, M.M., Trivedi. J.R., Krishnaswami, S., Sharma, K.K. 1994. The Indus river system (India-Pakistan): major ion chemistry, uranium and strontium isotopes. Chem Geol 116, 245–259.

Pauwels, H., Négrel, Ph., Dewandel, B., Perrin, J., Mascré, C., Roy, S., Ahmed, S., 2015. Hydrochemical borehole loggings for characterizing fluoride contamination in a heterogenous aquifer (Maheshwaram, India). J. Hydrol, 525, 302-312.

Perrin, J., Mascré, C., Pauwels, H., Ahmed, S., 2011. Solute recycling: an emerging threat to groundwater resources in southern India, J. Hydrol. 398, 144-154.

Petelet, E.: 1998, Application de la géochimie à l'étude des mouvements d'eaux à moyenne et petite échelle : les bassins versants de l'Hérault et de la Peyne (S. France). Utilisation des éléments majeurs, traces et des isotopes du Sr et du Pb. Ph.D. Dissertation, Université Montpellier II, France, pp. 512.

Pett-Ridge, J. C., Derry, L. A., Kurtz, A. C. 2009. Sr isotopes as a tracer of weathering processes and dust inputs in a tropical granitoid watershed, Luquillo Mountains, Puerto Rico. Geochim.Cosmochim. Acta, 73, 25-43.

Pierret, M.C, Stille, P., Prunier, J., Viville, D., Chabaux, F. 2014. Chemical and U–Sr isotopic variations in stream and source waters of the Strengbach watershed (Vosges mountains, France). Hydrol. Earth Syst. Sci. 18, 3969-3985.

Probst, A., El Gh'mari, A., Aubert, D., Fritz, B., McNutt, R. 2000. Strontium as a tracer of weathering processes in a silicate catchment polluted by acid atmospheric inputs, Strenbach, France. Chem. Geol. 170, 203–219.

Prunier, J., Chabaux, F., Stille, P., Ganglof, S., Pierret, M.C., Viville, D., Aubert, A. 2015. Geochemical and isotopic (Sr, U) monitoring of soil solutions from the Strengbach catchment (Vosges mountains, France): Evidence for recent weathering evolution. Che. Geol. 417, 289–305.

Roy, S., Gaillardet, J., Allegre, C.J. 1999, 'Geochemistry of dissolved and suspended loads of the Seine river, France: Anthropogenic impacts, carbonate and silicate weathering', Geochim. Cosmochim. Acta 63, 1277–1292.

Schaffhauser, T., Chabaux, F., Ambroise, B., Lucas, Y., Stille, P., Reuschlé, T., Perrone, T., Fritz, B. 2014. Geochemical and isotopic (U, Sr) tracing of water pathways in the granitic Ringelbach catchment (Vosges Mountains, France). Chem. Geol. 374–375, 117–127.

Seimbille, F., Négrel, Ph., Dupré, B. Allègre, C J. 1991. Geochemical study of a granitic watershed: What kind of information can the isotopic strontium ratio tool provide? Frontiers in Isotope Geosciences, Keyworth, U.K., 1991. Terra Abstracts 3, 11.

Semhi, K., Clauer, N. Probst, J.L. 2000. Strontium isotope compositions of river waters as records of lithology-dependent mass transfers: the Garonne river and its tributaries (SW France).

Singh, S.K., Trivedi, J.R., Pande, K., Ramesh, R., Krishnaswami, S. 1998. Chemical and strontium, oxygen, and carbon isotopic compositions of carbonates from the Lesser Himalaya: implications to the strontium isotope composition of the source waters of the Ganga, Ghaghara, and the Indus rivers. Geochim Cosmochim Acta 62:743–755.

Tricca, A., Stille, P., Steinmann, M., Kiefel, B., Samuel, J., Eikenberg, J. 1999. Rare earth elements and Sr and Nd isotopic compositions of dissolved and suspended loads from small river systems in the Vosges mountains (France), the river Rhine and groundwater. Chemical Geology, 160(1), 139-158. Chemical Geology 168. 173–193.

Wyns, R., Baltassat, J.M., Lachassagne, P., Legchenko, A., Vairon, J., Mathieu, F. 2004. Application of proton magnetic resonance soundings to groundwater reserve mapping in weathered basement rocks (Brittany, France). Bull. Soc. Geol. Fr. 175, 21-34.

Figure captions

Fig. 1. Conceptual model of hydrogeological properties in weathered basement rock, i.e.the hard rock aquifer concept, modified from Wyns et al. (2004).

Fig. 2. Map of the site locations of studied crystalline catchments in France (modified from Négrel and Pauwels, 2004).

Fig. 3. Map of the site locations: (a) India(Subarnarekha, Négrel et al., 2007,Maheshwaram, Négrel et al., 2010; Pauwels et al., 2015) and Himalayan rivers (Bothe Kosi River, Harris et al., 1998; Ganges headwaters, Bickle et al., 2005), (b) French Guiana (Négrel and Petelet-Giraud, 2010), Africa (Congo and Oubangui Rivers, Négrel et al., 1993; 1995a, b).

Fig. 4. Location of the study area in Andhra Pradesh (India) and simplified geological map of the Maheshwaram hydrosystem with location of sampled boreholes (Mxx for agricultural used boreholes and IFPX for scientific used boreholes).

Fig. 5. Sr *vs.* Mg contents (all µmol/l) in surface and groundwater interacting with silicate in France, modified from Négrel and Pauwels (2004).

Fig.6. Sr isotope ratios *vs.* Mg/Sr ratios modified from Négrel and Pauwels (2004) and additional data from the literature covering waters interacting with silicate in France.

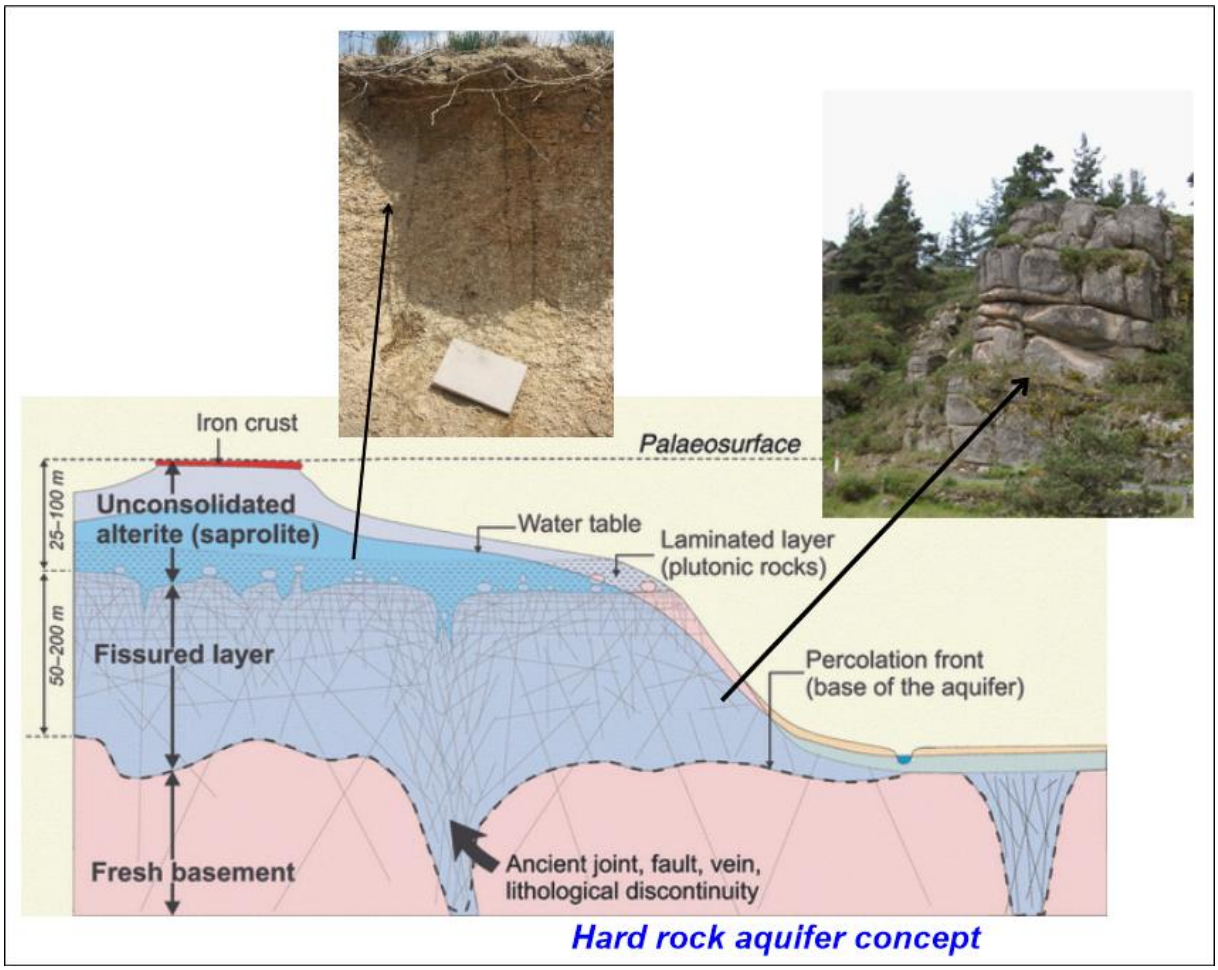
Fig.7. (a) Plot of the $^{87}Sr/^{86}Sr$ *vs.* Cl concentration expressed in µmol/l for the groundwater samples collected in the Maheshwaram hydrosystem in 2006 (A. Dayal, personal communication) and 2008 (this study); (b) plot of $^{87}Sr/^{86}Sr$ *vs.* 1/Sr (Sr concentration expressed in µmol/l).

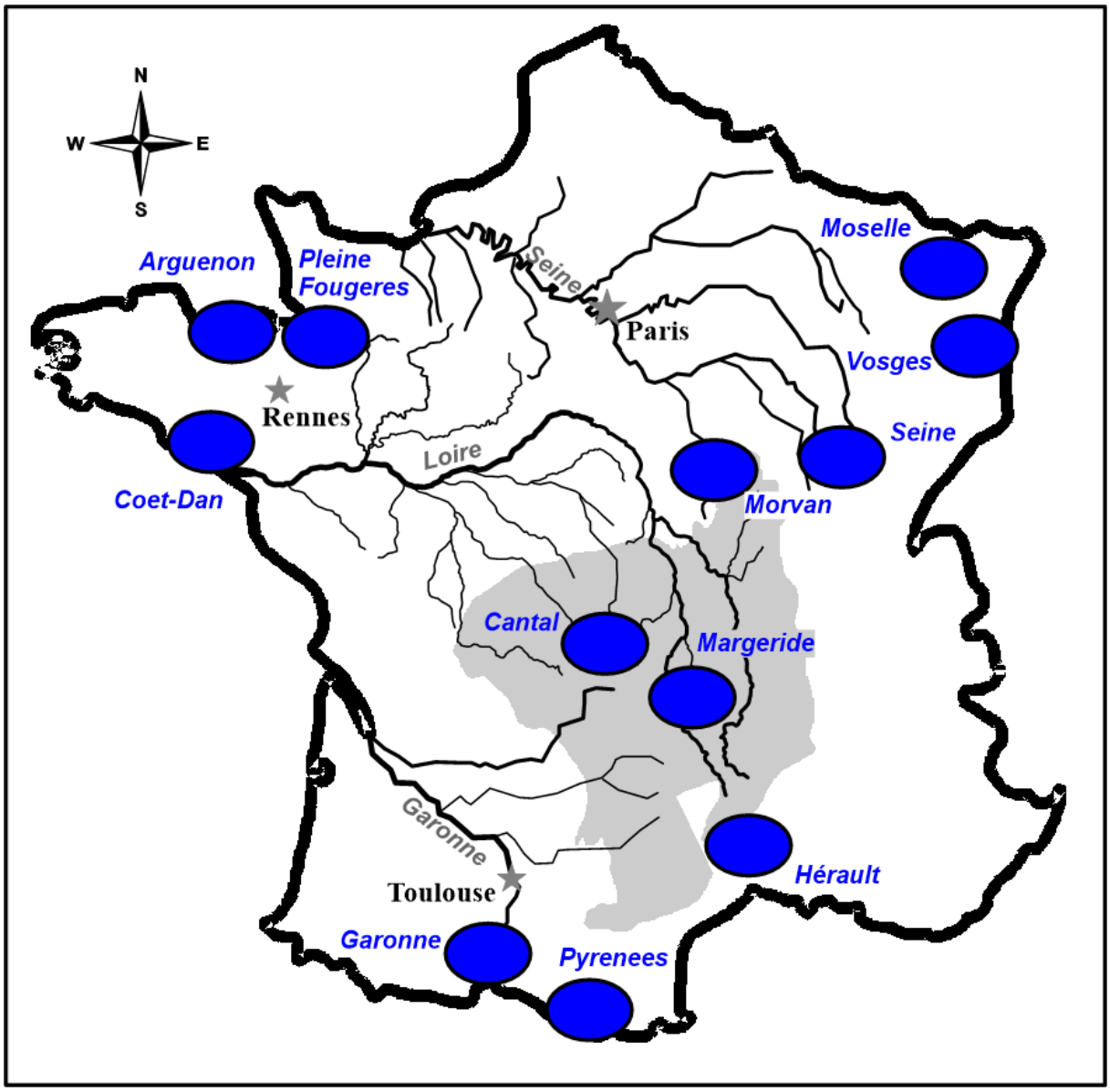
Fig. 8. Sr *vs.* Mg contents (all µmol/l) when enlarging to worldwide basins and catchments in Africa (Congo Basin Négrel et al. 1993; Orange River; de Villiers et al., 2000); India and Nepal (Négrel et al., 2007a and this study for India; Himalaya metamorphic, silicate metasediments and gneisses 630 to 490 Ma; Harris et al., 1998; Bickle et al., 2005); North America (3500 to 2500 Ma silicate rocks in the Mackenzie basin; Millot et al., 2002 and 1000 to 70 Ma silicate rocks in the Fraser Basin in Canada; Cameron et al., 1995 and 1760 to 1430 anorthosite and granite in the Laramie aquifer in Wyoming; Frost and Toner, 2004); South America in French Guiana (Archaen gneiss 3400 to 2700 Ma and granite-gneiss rocks 2300 to 1900 Ma; Négrel and Petelet-Giraud, 2010); Australia (65 Ma arenaceous and argillaceous rocks; and considering both surface and groundwater; Harrington and Herczeg, 2003).

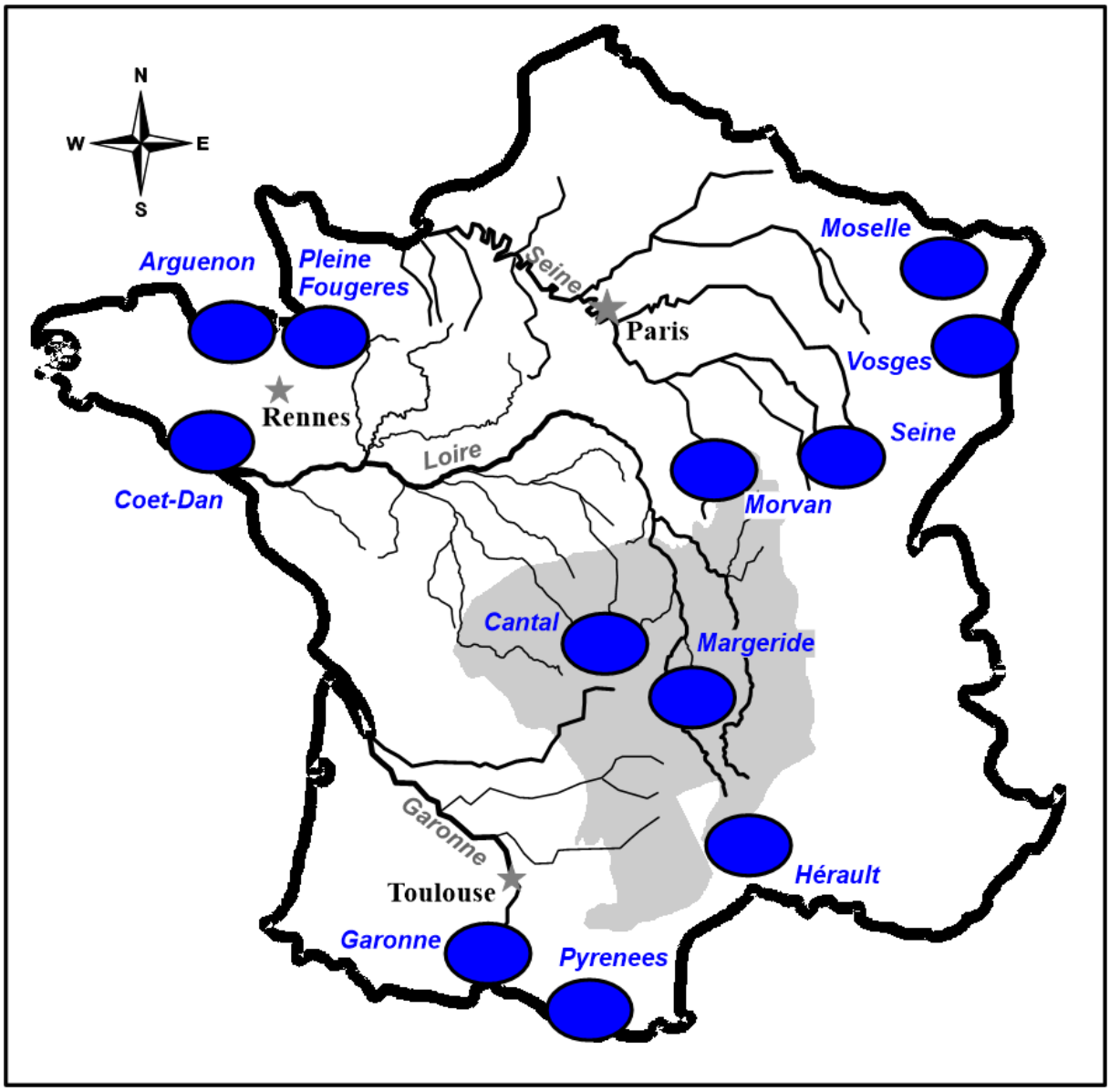
Fig. 9. Sr isotope ratios *vs.* Mg/Sr ratios, modified from Fig. 6, and additional data when enlarging to worldwide basins and catchments in Africa (Congo Basin Négrel et al. 1993; Orange River; de Villiers et al., 2000); India and Nepal (Négrel et al., 2007a and this study for India; Himalaya metamorphic, silicate metasediments and gneisses 630 to 490 Ma; Harris et al., 1998; Bickle et al., 2005); North America (3500 to 2500 Ma silicate rocks in the Mackenzie basin; Millot et al., 2002 and 1000 to 70 Ma silicate rocks in the Fraser Basin in Canada; Cameron et al., 1995 and 1760 to 1430 anorthosite and granite in the Laramie aquifer in Wyoming; Frost and Toner, 2004); South America in French Guiana (Archaen gneiss 3400 to 2700 Ma and granite-gneiss rocks 2300 to 1900 Ma; Négrel and Petelet-Giraud, 2010); Australia (65 Maarenaceous and argillaceous rocks; and considering both surface and groundwater; Harrington and Herczeg, 2003).

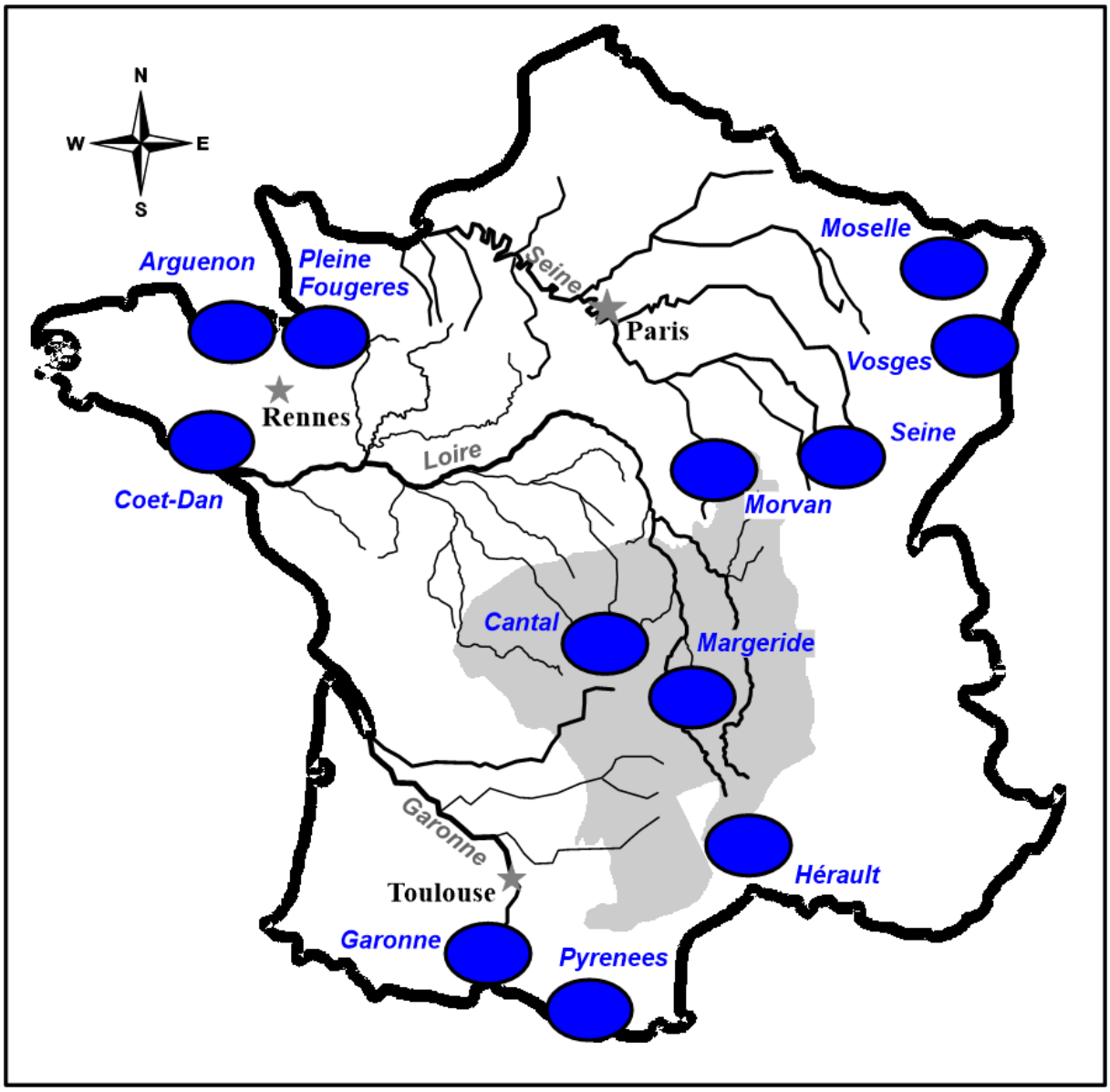
Table captions

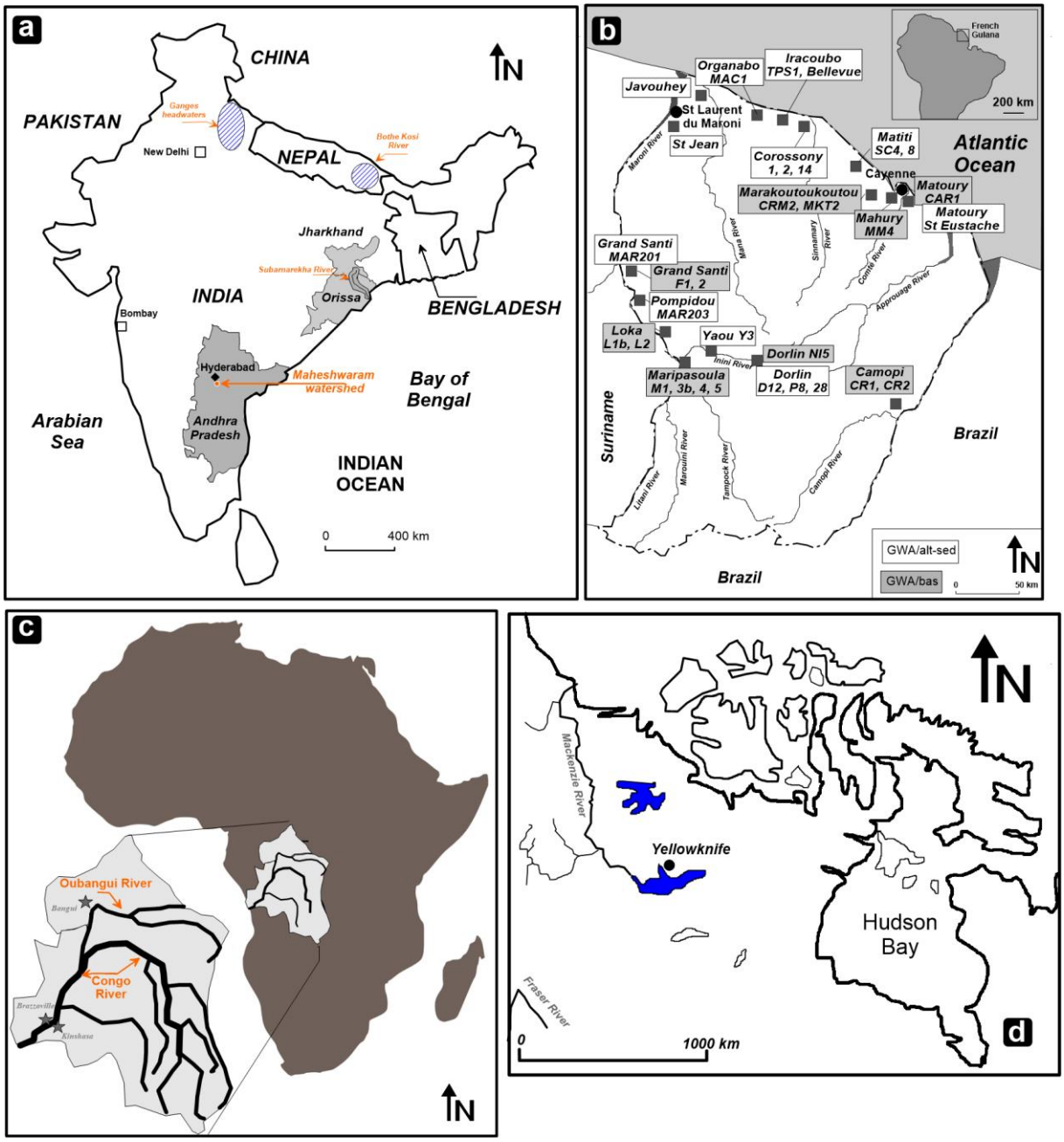
Table 1. Mg and Sr concentration expressed in µmol/l, $^{87}Sr/^{86}Sr$ ratios for the groundwater samples collected in the Maheshwaram hydrosystem in 2006 (A. Dayal, personal communication) and 2008 (this study).

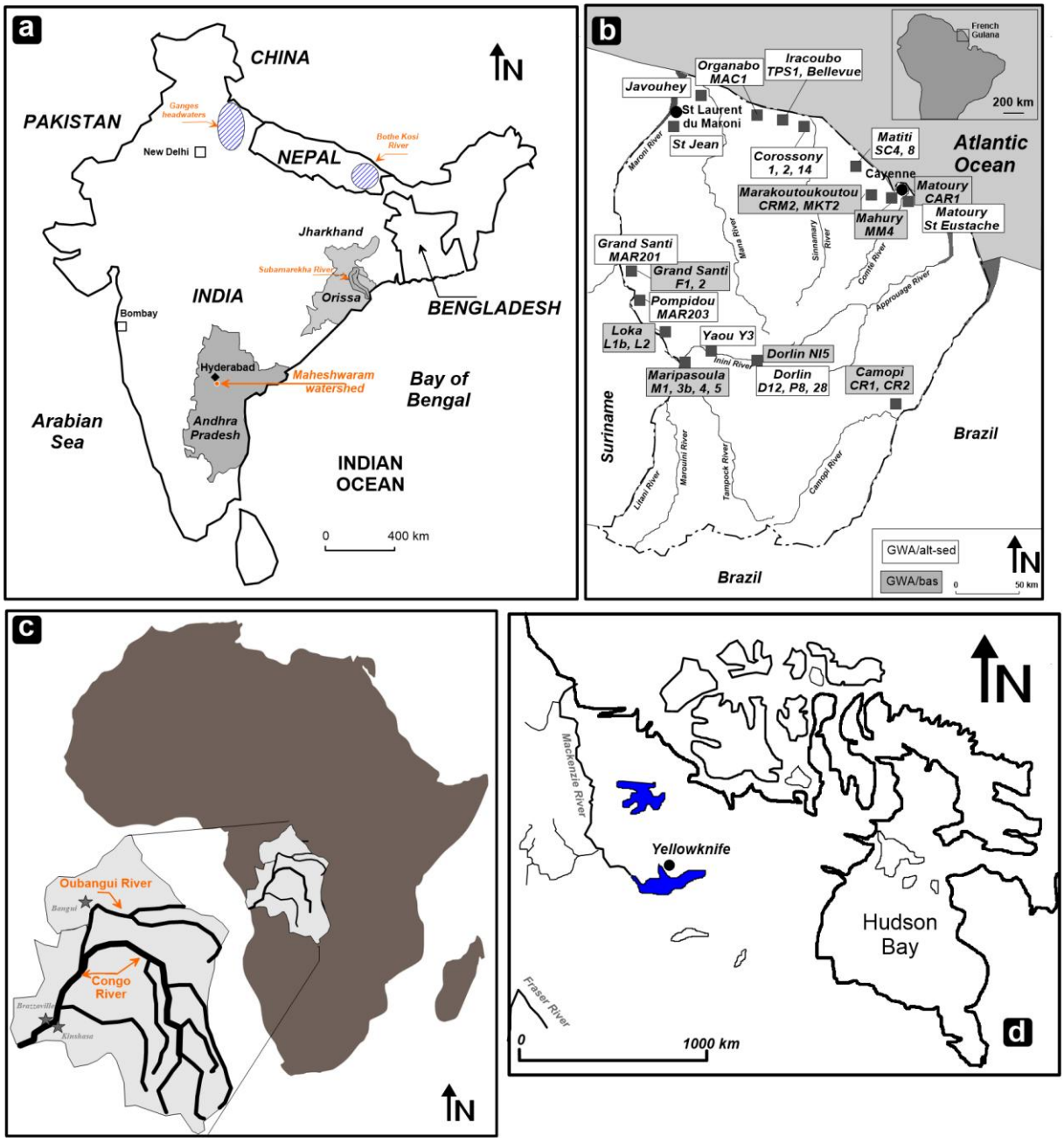

Iron crust
Palaeosurface
25–100 m
Unconsolidated
alterite (saprolite)
Water table
Laminated layer
(plutonic rocks)
50–200 m
Fissured layer
Percolation front
(base of the aquifer)
Fresh basement
Ancient joint, fault, vein,
lithological discontinuity
Hard rock aquifer concept

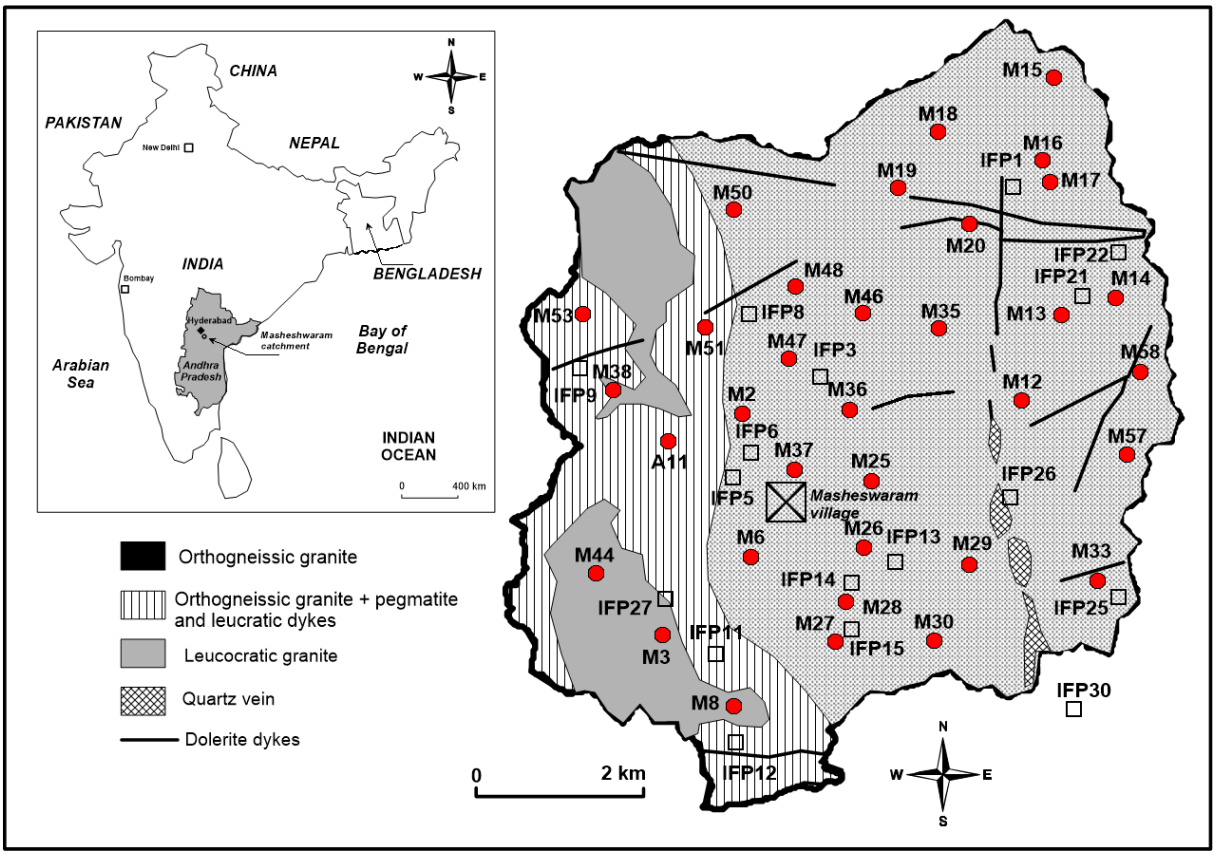

N
W
E
S
Arguenon
Pleine
Fougeres
Seine
Moselle
Paris
Vosges
Rennes
Loire
Seine
Coet-Dan
Morvan
Cantal
Margeride
Garonne
Hérault
Toulouse
Garonne
Pyrenees

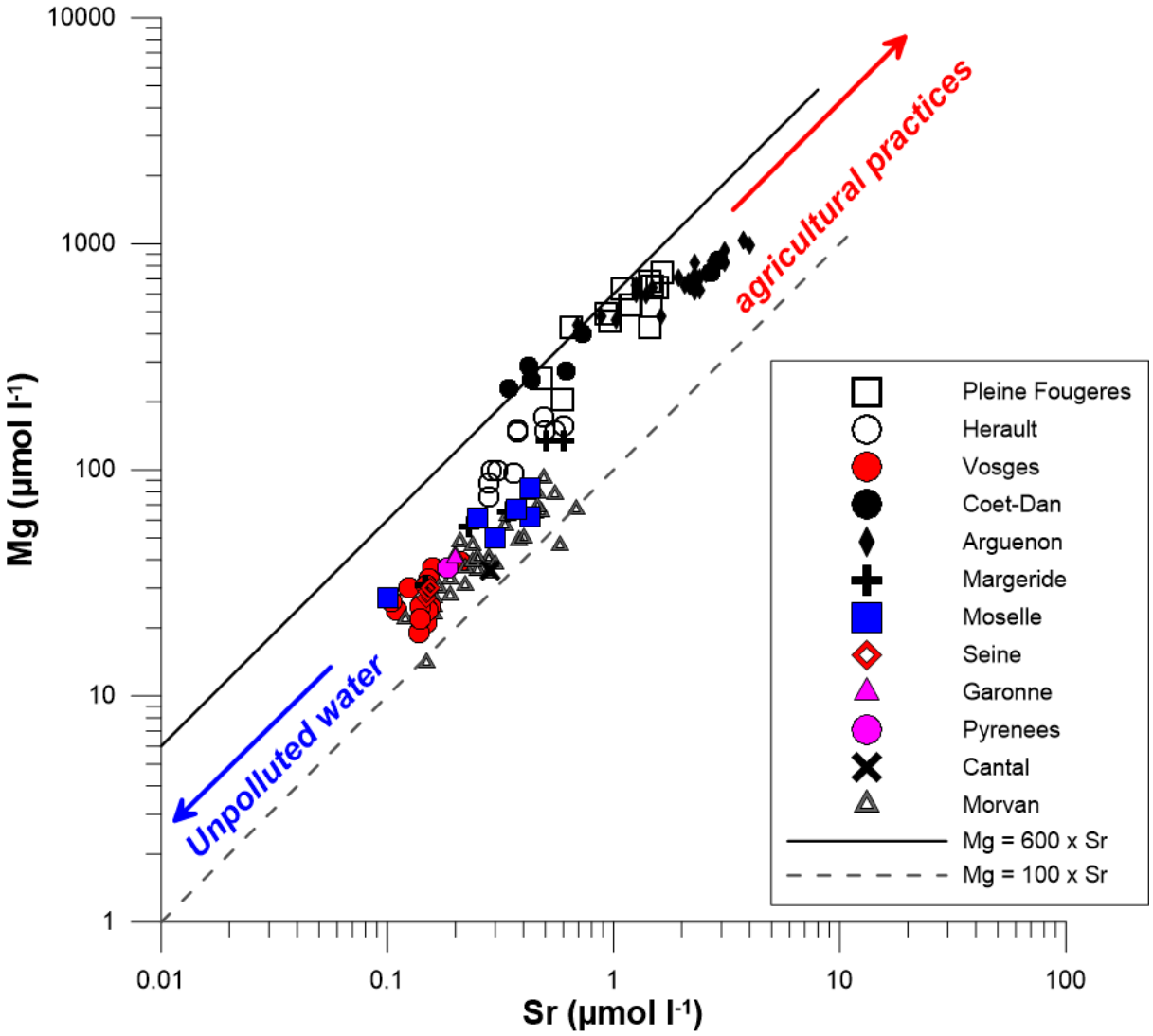

N
W
E
S
Arguenon
Pleine
Fougeres
Seine
Moselle
Paris
Vosges
Rennes
Seine
Loire
Coet-Dan
Morvan
Cantal
Margeride
Garonne
Hérault
Toulouse
Garonne
Pyrenees

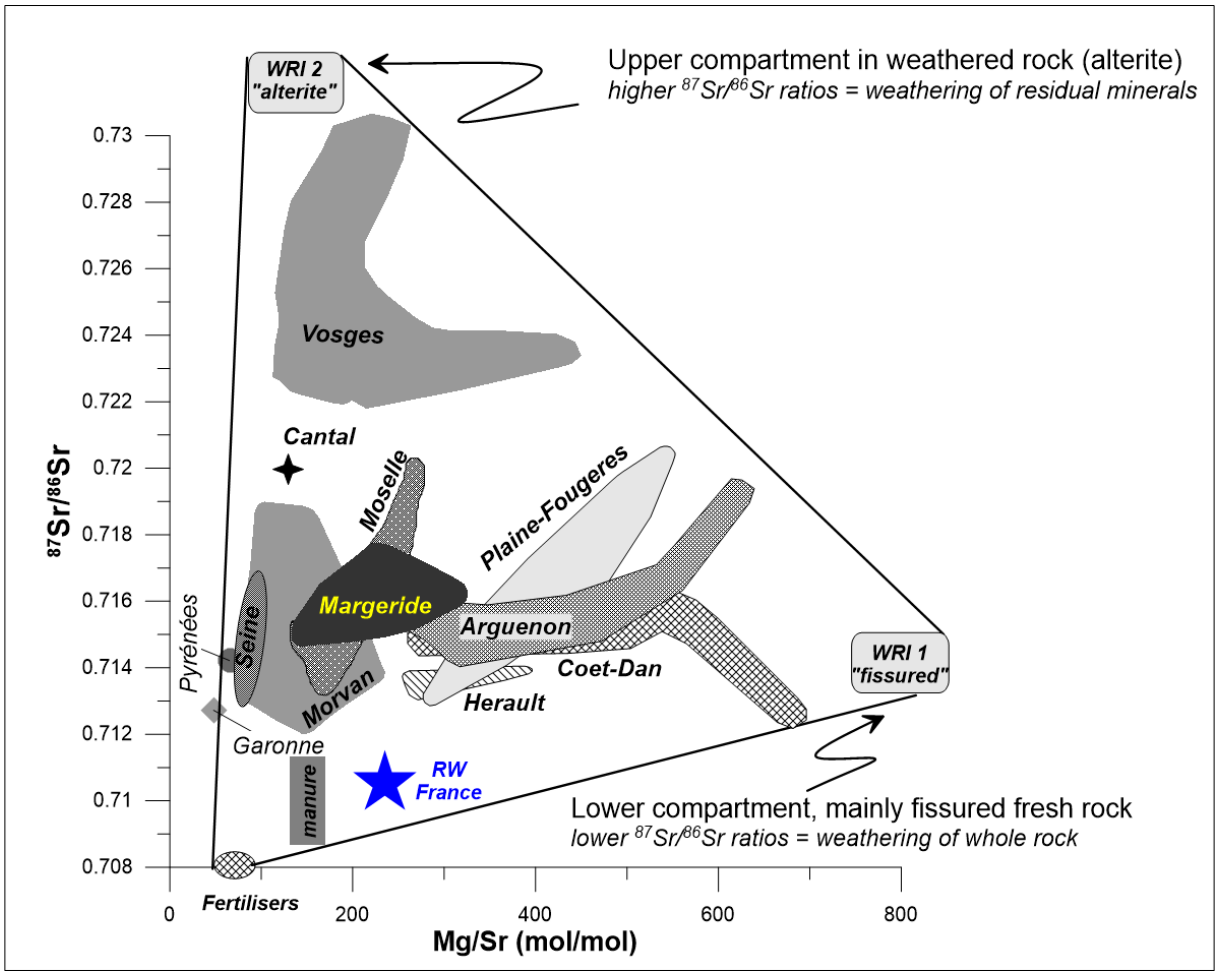

N
W
E
S
Arguenon
Pleine
Fougeres
Seine
Paris
Moselle
Vosges
Rennes
Loire
Seine
Coet-Dan
Morvan
Cantal
Margeride
Garonne
Hérault
Toulouse
Garonne
Pyrenees

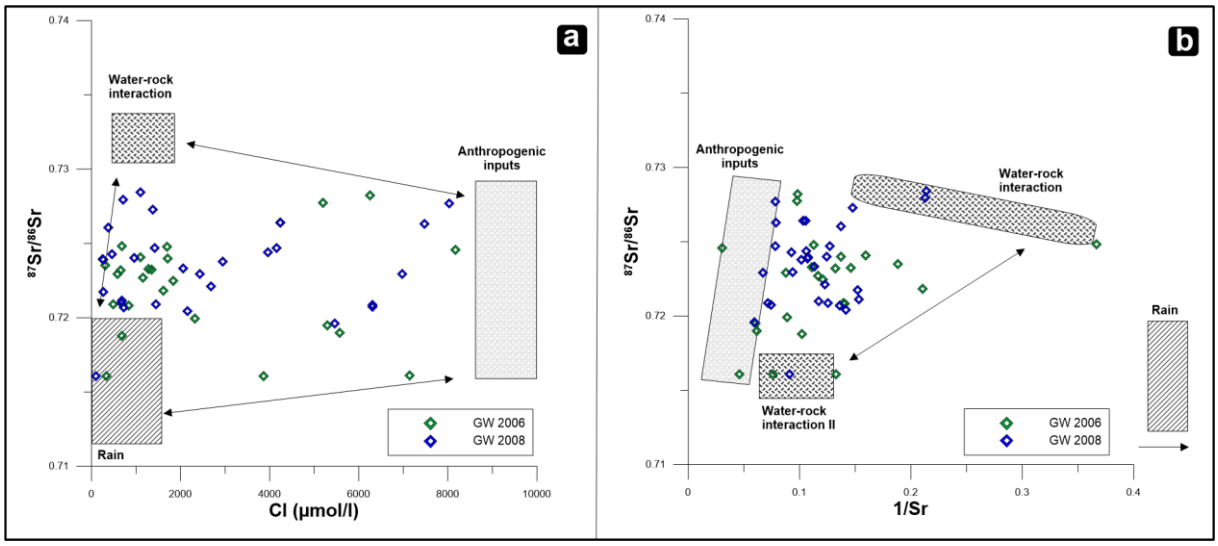

a
CHINA
N
PAKISTAN
Ganges headwaters
New Delhi
NEPAL
Bothe Kosi River
Jharkhand
Subamarekha River
INDIA
Orissa
BENGLADESH
Bombay
Hyderabad
Maheshwaram watershed
Bay of Bengal
Arabian Sea
Andhra Pradesh
INDIAN OCEAN
0
400 km
b
French Guiana
200 km
Organabo MAC1
Iracoubo TPS1, Bellevue
Javouhey
St Laurent du Maroni
St Jean
Maroni River
Matiti SC4, 8
Atlantic Ocean
Corossony 1, 2, 14
Cayenne
Matoury CAR1
Marakoutoukoutou CRM2, MKT2
Mahury MM4
Matoury St Eustache
Grand Santi MAR201
Grand Santi F1, 2
Mana River
Sinnamary River
Comté River
Approuague River
Pompidou MAR203
Loka L1b, L2
Yaou Y3
Dorlin NI5
Inini River
Maripasoula M1, 3b, 4, 5
Dorlin D12, P8, 28
Camopi CR1, CR2
Suriname
Brazil
Litani River
Marouini River
Tampock River
Camopi River
Brazil
GWA/alt-sed
GWA/bas
N
0
50 km
c
Oubangui River
Bangui
Congo River
Brazzaville
Kinshasa
N
d
N
Mackenzie River
Yellowknife
Hudson Bay
Fraser River
0
1000 km

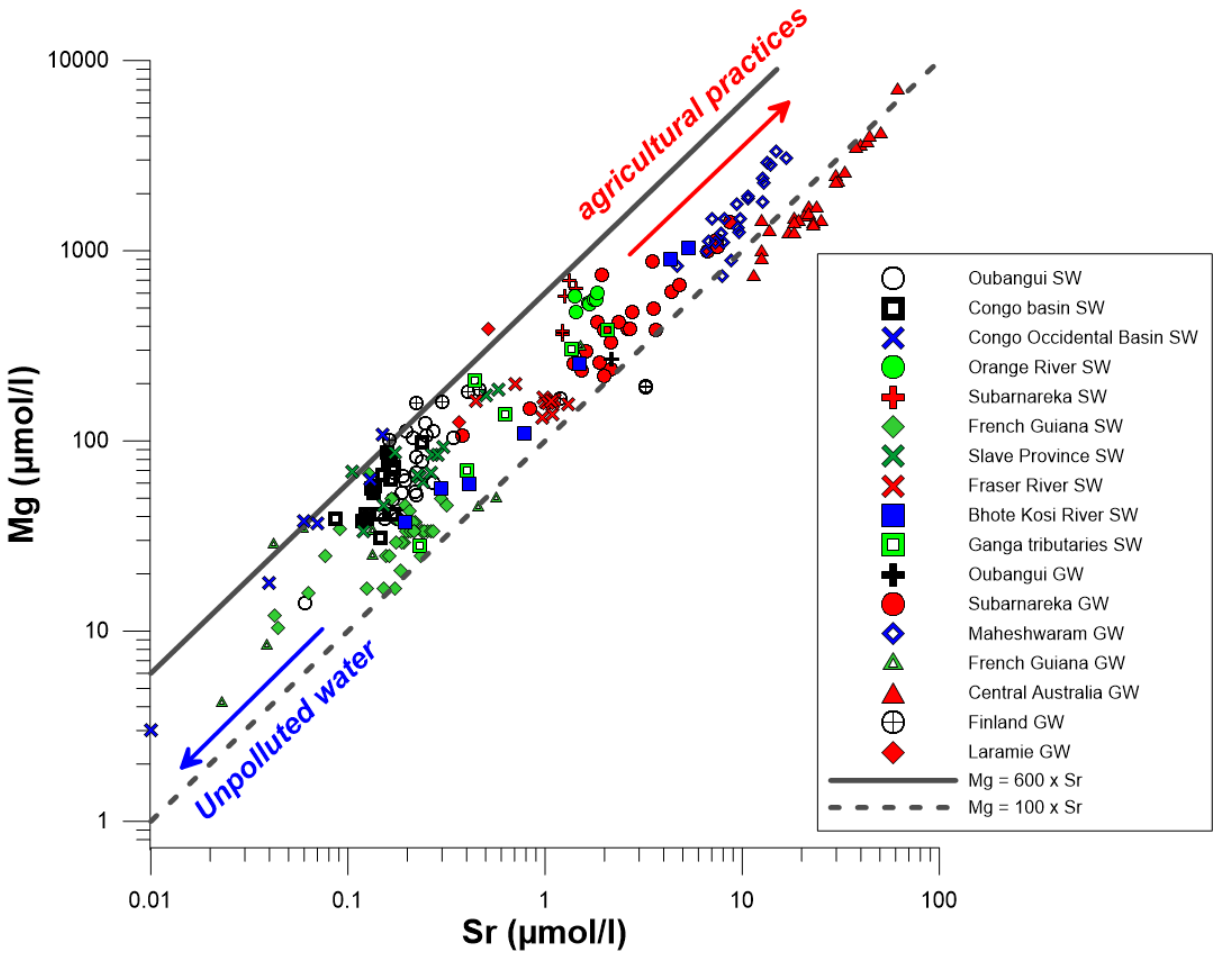

a
CHINA
N
PAKISTAN
Ganges headwaters
New Delhi
NEPAL
Bothe Kosi River
Jharkhand
Subamarekha River
INDIA
Orissa
BENGLADESH
Bombay
Hyderabad
Maheshwaram watershed
Bay of Bengal
Arabian Sea
Andhra Pradesh
INDIAN OCEAN
0
400 km
b
French Guiana
200 km
Organabo MAC1
Iracoubo TPS1, Bellevue
Javouhey
St Laurent du Maroni
St Jean
Maroni River
Matiti SC4, 8
Atlantic Ocean
Corossony 1, 2, 14
Cayenne
Matoury CAR1
Marakoutoukoutou CRM2, MKT2
Mahury MM4
Matoury St Eustache
Grand Santi MAR201
Grand Santi F1, 2
Mana River
Sinnamary River
Comté River
Approuague River
Pompidou MAR203
Loka L1b, L2
Yaou Y3
Dorlin NI5
Inini River
Maripasoula M1, 3b, 4, 5
Dorlin D12, P8, 28
Camopi CR1, CR2
Suriname
Brazil
Litani River
Marouini River
Tampock River
Camopi River
Brazil
GWA/alt-sed
GWA/bas
N
0
50 km
c
Oubangui River
Bangui
Congo River
Brazzaville
Kinshasa
N
d
N
Mackenzie River
Yellowknife
Hudson Bay
Fraser River
0
1000 km

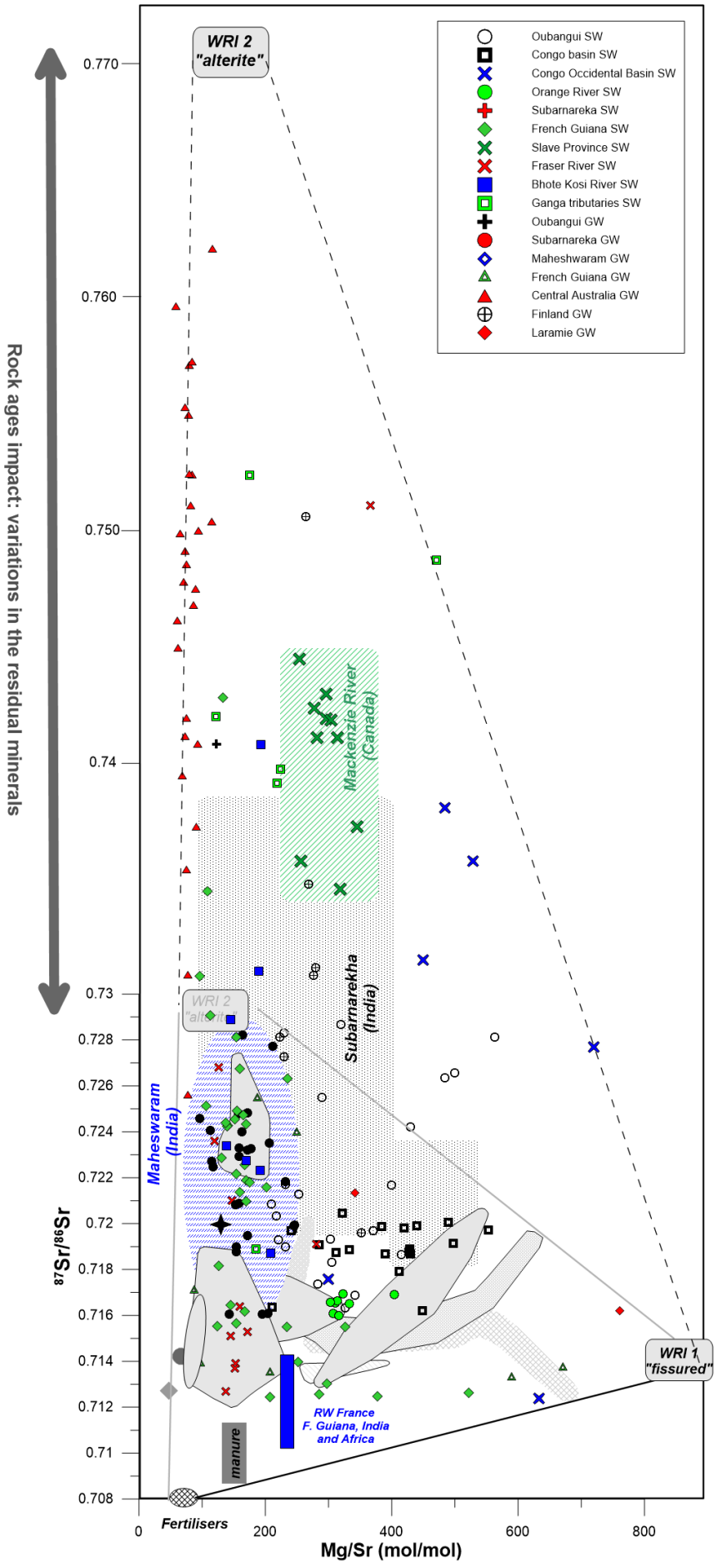

CHINA
PAKISTAN
NEPAL
New Delhi
INDIA
Bombay
BENGLADESH
Hyderabad
Masheshwaram catchment
Andhra Pradesh
Arabian Sea
Bay of Bengal
INDIAN OCEAN
0 400 km
N
W E
S
Orthogneissic granite
Orthogneissic granite + pegmatite and leucratic dykes
Leucocratic granite
Quartz vein
Dolerite dykes
M15
M18
M16
IFP1
M17
M19
M50
M20
IFP22
IFP21
M14
M48
M46
M35
M13
M53
IFP8
M51
M47
IFP3
M58
M38
IFP9
M2
M36
M12
IFP6
M37
M57
A11
M25
IFP26
IFP5
Masheswaram village
M6
M26
IFP13
M29
M33
M44
IFP14
IFP27
M28
IFP25
M27
M30
IFP11
IFP15
M3
IFP30
M8
IFP12
0 2 km
N
W E
S


10000
1000
100
10
1
Mg (µmol l-1)
0.01
0.1
1
10
100
Sr (µmol l-1)
agricultural practices
Unpolluted water
Pleine Fougeres
Herault
Vosges
Coet-Dan
Arguenon
Margeride
Moselle
Seine
Garonne
Pyrenees
Cantal
Morvan
Mg = 600 x Sr
Mg = 100 x Sr


WRI 2
"alterite"
Upper compartment in weathered rock (alterite)
higher 87Sr/86Sr ratios = weathering of residual minerals
0.73
0.728
0.726
0.724
0.722
0.72
0.718
0.716
0.714
0.712
0.71
0.708
87Sr/86Sr
Vosges
Cantal
Moselle
Plaine-Fougeres
Margeride
Seine
Pyrénées
Arguenon
Coet-Dan
Herault
Morvan
Garonne
WRI 1
"fissured"
manure
RW
France
Lower compartment, mainly fissured fresh rock
lower 87Sr/86Sr ratios = weathering of whole rock
Fertilisers
0
200
400
600
800
Mg/Sr (mol/mol)


a
Water-rock interaction
Anthropogenic inputs
Rain
GW 2006
GW 2008
$^{87}Sr/^{86}Sr$
Cl (µmol/l)
0.74
0.73
0.72
0.71
0
2000
4000
6000
8000
10000
b
Anthropogenic inputs
Water-rock interaction
Water-rock interaction II
Rain
GW 2006
GW 2008
$^{87}Sr/^{86}Sr$
1/Sr
0
0.1
0.2
0.3
0.4


agricultural practices
Unpolluted water
Mg (µmol/l)
Sr (µmol/l)
10000
1000
100
10
1
0.01
0.1
1
10
100
Oubangui SW
Congo basin SW
Congo Occidental Basin SW
Orange River SW
Subarnareka SW
French Guiana SW
Slave Province SW
Fraser River SW
Bhote Kosi River SW
Ganga tributaries SW
Oubangui GW
Subarnareka GW
Maheshwaram GW
French Guiana GW
Central Australia GW
Finland GW
Laramie GW
Mg = 600 x Sr
Mg = 100 x Sr


Rock ages impact: variations in the residual minerals
WRI 2
"alterite"
WRI 1
"fissured"
Oubangui SW
Congo basin SW
Congo Occidental Basin SW
Orange River SW
Subarnareka SW
French Guiana SW
Slave Province SW
Fraser River SW
Bhote Kosi River SW
Ganga tributaries SW
Oubangui GW
Subarnareka GW
Maheshwaram GW
French Guiana GW
Central Australia GW
Finland GW
Laramie GW
Mackenzie River (Canada)
Subarnarekha (India)
Maheswaram (India)
RW France
F. Guiana, India
and Africa
manure
Fertilisers
87Sr/86Sr
Mg/Sr (mol/mol)
0.770
0.760
0.750
0.74
0.73
0.728
0.726
0.724
0.722
0.72
0.718
0.716
0.714
0.712
0.71
0.708
0
200
400
600
800

Sample	Mg µmol	Sr µmol	$^{87}Sr/^{86}Sr$		Sample	Mg µmol	Sr µmol	$^{87}Sr/^{86}Sr$
2006	µmol/L	µmol/L			***2008***	µmol/L	µmol/L	
IFP 12	1747	10.1	0.728226		M2	2404	12.7	0.726301
A11	1145	7.1	0.72083		M3	888	8.8	0.723328
HP3	4664	21.8	0.716094		M6	1105	8.0	0.724011
M03	1041	8.6	0.722701		M8	739	8.0	0.720892
M06	1496	9.0	0.723293		M12	1101	7.4	0.720694
M08	740	6.3	0.724064		M30	999	6.6	0.721741
M12	1583	9.8	0.718774		M35	1877	10.7	0.722948
M13	2674	13.1	0.71606		M48	1241	7.9	0.724700
M15	3337	33.0	0.724582		M50	1114	6.8	0.727282
M17	2964	16.5	0.719486		M51	2272	12.8	0.727688
M18	2628	16.3	0.718987		M53	1935	10.8	0.724285
M20	1155	4.7	0.72183		M57	3065	16.8	0.719595
M25	1192	7.2	0.720891		IFP1/1	1474	7.1	0.720433
M26	1895	11.4	0.722921		IFP1/1a	1481	8.1	0.722106
M27	1362	7.6	0.723186		IFP1/7	2910	13.5	0.720743
M30	1146	5.3	0.723503		IFP1/7a	2821	13.9	0.720857
M33	1130	7.5	0.71606		IFP1/7b	3335	14.8	0.722931
M35	1272	6.8	0.723252		IFP5	1478	9.8	0.723768
M38B	1244	7.3	0.723981		IFP6	1747	9.4	0.724389
M44	1460	8.9	0.724783		IFP6	1813	12.8	0.724689
M46	1014	8.3	0.722471		IFP8	1316	9.5	0.726401
M48	490	2.7	0.724826		IFP8	1248	9.7	0.726405
M51	2265	10.2	0.727728		IFP9	836	4.7	0.728431
M58	2895	11.2	0.719925		IFP9	785	4.7	0.727958
					IFP13	1228	9.3	0.723954
					IFP14	1060	7.3	0.726056
					IFP15	1093	8.5	0.721001
					IFP25	1572	11.0	0.716063

Table 1